The Plant Cell, Vol. 25: 2573–2586, July 2013, www.plantcell.org

An *Arabidopsis* ATP-Dependent, DEAD-Box RNA Helicase Loses Activity upon IsoAsp Formation but Is Restored by PROTEIN ISOASPARTYL METHYLTRANSFERASE[C][W]

Nihar R. Nayak,[a,b,1] Andrea A. Putnam,[c] Balasubrahmanyam Addepalli,[d] Jonathan D. Lowenson,[e] Tingsu Chen,[a,b,2] Eckhard Jankowsky,[c] Sharyn E. Perry,[b,f] Randy D. Dinkins,[g] Patrick A. Limbach,[d] Steven G. Clarke,[e] and A. Bruce Downie[a,b,3]

[a] Department of Horticulture, University of Kentucky, Lexington, Kentucky 40546-0312
[b] Seed Biology Group, University of Kentucky, Lexington, Kentucky 40546-0312
[c] Center for RNA Molecular Biology and Department of Biochemistry, Case Western Reserve University, School of Medicine, Cleveland, Ohio 44106
[d] Department of Chemistry, University of Cincinnati, Cincinnati, Ohio 45221
[e] Department of Chemistry and Biochemistry, University of California, Los Angeles, California 90095-1569
[f] Department of Plant and Soil Sciences, University of Kentucky, Lexington, Kentucky 40546-0312
[g] U.S. Department of Agriculture–Agricultural Research Service Forage Animal Production Research Unit, N220C Agriculture Science Center North, University of Kentucky, Lexington, Kentucky 40546-0312

ORCID IDs: 0000-0003-1526-4546 (P.A.L.); 0000-0002-7303-6632 (S.G.C.); 0000-0001-6680-0551 (A.B.D.).

Orthodox seeds are capable of withstanding severe dehydration. However, in the dehydrated state, Asn and Asp residues in proteins can convert to succinimide residues that can further react to predominantly form isomerized isoAsp residues upon rehydration (imbibition). IsoAsp residues can impair protein function and can render seeds nonviable, but PROTEIN ISOASPARTYL METHYLTRANSFERASE (PIMT) can initiate isoAsp conversion to Asp residues. The proteins necessary for translation upon imbibition in orthodox seeds may be particularly important to maintain in an active state. One such protein is the large, multidomain protein, *Arabidopsis thaliana* PLANT RNA HELICASE75 (PRH75), a DEAD-box helicase known to be susceptible to isoAsp residue accumulation. However, the consequences of such isomerization on PRH75 catalysis and for the plant are unknown. Here, it is demonstrated that PRH75 is necessary for successful seed development. It acquires isoAsp rapidly during heat stress, which eliminates RNA unwinding (but not rewinding) competence. The repair by PIMT is able to restore PRH75's complex biochemical activity provided isoAsp formation has not led to subsequent, destabilizing conformational alterations. For PRH75, an important enzymatic activity associated with translation would be eliminated unless rapidly repaired by PIMT prior to additional, deleterious conformational changes that would compromise seed vitality and germination.

INTRODUCTION

Orthodox seeds are capable of withstanding dehydration to ~5% moisture content fresh weight (Roberts, 1973), then entering a period of quiescence that can maintain viability for centuries in some species (Shen-Miller et al., 1995; Sallon et al., 2008). This capacity forms the basis of agriculture, allowing a portion of harvested seed to be retained to produce next season's crop. In this partially dehydrated state, proteins can undergo spontaneous degradation to form the succinimide derivative of Asn and Asp residues (Desfougères et al., 2011) that is then largely converted to the isomerized isoAsp derivative upon imbibition. IsoAsp formation is often detrimental to proper protein function and, if unrepaired, can be lethal (Ogé et al., 2008; Verma et al., 2013).

Using phage display and affinity selection with recombinant *Arabidopsis thaliana* PROTEIN ISOASPARTYL METHYLTRANSFERASE (rPIMT1), isoAsp-susceptible proteins present in mature, dehydrated, or germinating seeds were identified, a disproportionate number of which were found to be involved in translation (Chen et al., 2010). From these and other data (Rajjou et al., 2004, 2008, 2012; Kimura and Nambara, 2010; An and Lin, 2011; He et al., 2011; Kushwaha et al., 2012), it has been hypothesized that the proteins of the translational machinery could be viewed as an Achilles heel of orthodox seed longevity (Kushwaha et al., 2013) and may be a major target requiring protection and PIMT-mediated repair in organisms capable of entering a period of quiescence. One such target of rPIMT1 was PLANT RNA HELICASE75 (PRH75), a presumptive ATP-

[1] Current address: Regional Plant Resource Centre, Nayapalli, Bhubaneswar, Odisha 751015, India.
[2] Current address: Microbiology Institute, Guangxi Academy of Agricultural Sciences, Daxue East-Road 174, Nanning Guangxi 530007, People's Republic of China.
[3] Address correspondence to adownie@uky.edu.
The author responsible for distribution of materials integral to the findings presented in this article in accordance with the policy described in the Instructions for Authors (www.plantcell.org) is: A. Bruce Downie (adownie@uky.edu).
[C] Some figures in this article are displayed in color online but in black and white in the print edition.
[W] Online version contains Web-only data.
www.plantcell.org/cgi/doi/10.1105/tpc.113.113456

dependent, DEAD-box, RNA helicase (EC 3.6.4.13) targeted to the nucleolus and presumably involved in translation by assisting ribosome maturation (Lorković et al., 1997, 2004). The protein shares considerable sequence similarity with the mung bean (*Vigna radiata*) RNA HELICASE1, which was isolated as a differentially expressed cDNA noticeably more abundant in artificially aged (but viable) seeds relative to unaged seeds just following the completion of germination (Li et al., 2001). Although the accumulation of isoAsp in PRH75 was documented (Chen et al., 2010), the consequences of isoAsp formation in this enzyme remains unknown.

Here, we demonstrate that PRH75 has an ATP-dependent RNA unwinding activity that can be rapidly compromised by thermal insult, a treatment known to result in isoAsp formation (Chen et al., 2010). An analysis of liquid chromatography–tandem mass spectrometry (LC-MS/MS) tryptic fragments of recombinant, thermally insulted, PRH75 protein identified both of the Asp residues in motif II (DEAD) as capable of isoAsp formation. PRH75 activity can be rescued in vitro by recombinant PIMT and *S*-adenosyl Met (AdoMet), the enzyme's methyl-donating cofactor, if the duration of heat treatment has not exceeded 4 h. Severe mutations in *PRH75* are lethal during embryogenesis, indicating that considerable declines in PRH75 enzymatic capacity have dire consequences for the plant. Because the DEAD-motif is conserved among a large group of superfamily II RNA helicases across phylogenetic kingdoms, it is possible that the DEAD-box RNA helicases in general are susceptible to isoAsp formation, requiring PIMT to chaperone the regeneration of functional protein, a process particularly important in those organisms capable of anhydrobiosis.

RESULTS

PRH75 Is an ATP-Dependent RNA Helicase

PRH75 has 13 motifs associated with DEAD-box RNA helicases (Bork and Koonin, 1993; Koonin, 1993; Rocak and Linder, 2004; Jankowsky and Putnam, 2010) (see Supplemental Figure 1A online). Through its homology with RNA helicases in spinach (*Spinacia oleracea*) and mung bean (Lorković et al., 1997; Li et al., 2001), PRH75 has been assumed to be an ATP-dependent, DEAD-box RNA helicase. However, the non-translocating DEAD-box family of RNA binding proteins are not all helicases, regardless of the presence of the motifs mentioned above (Pyle, 2008). Furthermore, only a few DEAD-box proteins that have been tested demonstrate RNA unwinding activity with a generic RNA duplex substrate (Rocak and Linder, 2004; Cordin et al., 2006). Additionally, the presence of an Arg/Gly-rich C-terminal extension on PRH75 suggested, but did not demonstrate, a strand rewinding capacity (Yang et al., 2007). If the consequences of isoAsp formation on PRH75 enzymatic function are to be examined, it was imperative to demonstrate that the extrapolation of PRH75's function, based on structural similarity and motif presence, was valid (Jankowsky and Fairman, 2007).

An RNA duplex was stable under reaction conditions, without PRH75 (Figure 1A). No unwinding was seen with PRH75 without ATP (Figure 1B). Unwinding was observed with both PRH75 and ATP, and increasing amounts of enzyme increased the observed unwinding rate (Figures 1C to 1E). PRH75 also demonstrated a modest RNA rewinding capacity, which has been observed for other DEAD-box helicases (Jankowsky and Putnam, 2010), and is consistent with predictions based on its C-terminal sequence (see Supplemental Figures 2A to 2C online).

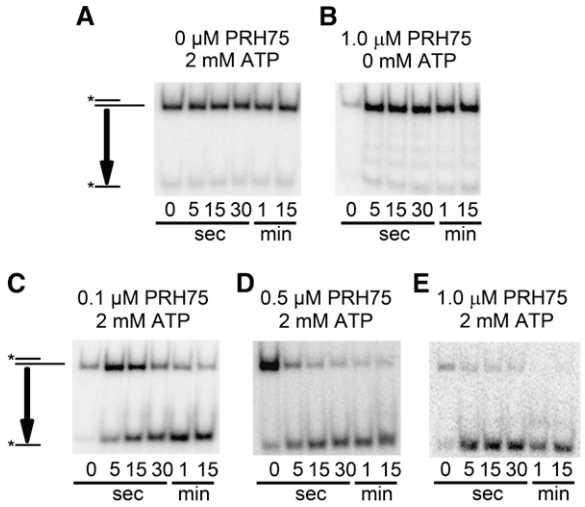

Figure 1. PRH75 Is an ATP-Dependent RNA Helicase.

Double-stranded RNA was stable in the presence of 2 mM ATP without recombinant PRH75 **(A)** or with PRH75 but no ATP **(B)**. Three different concentrations of PRH75 influenced the completeness with which double-stranded RNA template was converted to single-stranded product: 0.1 μM PRH75 **(C)**, 0.5 μM PRH75 **(D)**, and 1 μM PRH75 **(E)**. The asterisk on the depiction of the short strand of the RNA duplex represents the radio-labeled phosphate.

Detection of IsoAsp in PRH75 Exposed to Thermal Insult

PRH75 has been previously demonstrated to accumulate PIMT-methylatable isoAsp due to thermal insult using PIMT enzyme assays (Chen et al., 2010). The formation and location of isoAsp residues in PRH75 were examined directly by comparing tryptic peptides of preexposed (to 25 or 37°C for 4, 12, 24, and 36 h) protein using electron transfer dissociation (ETD)–based LC-MS/MS analysis. Irrespective of the temperature to which PRH75 had been exposed, this analysis yielded ~35 to 40% sequence coverage (see Supplemental Figures 1A and 1B online) of PRH75 with a consistent appearance of the DEAD-box-associated tryptic peptide ^{253}VLDEADEMLR^{262}. ETD is generated by ion–ion interactions between multiply charged positive ions (peptides in this case) and negatively charged fluoranthene anions leading to radical-based rearrangements and cleavage of N-C_α bonds in peptides. In isoaspartyl-containing peptides, the C_α-C_β bond is cleaved to generate two diagnostic backbone fragments at c_n +57 (or c_n+58) and $z_{(l-n)+1}$ −57. The latter fragment ion defines both the presence and the position of the isoAsp residue (O'Connor et al., 2006).

The MS/MS spectra of the tryptic peptide VLDEADEMLR showed predominantly z-type fragment ions with few or no

c-type fragment ions, presumably because of the location of positively charged amino acids at the C-terminal end. Incubation of PRH75 at 25°C for 36 h did not cause any apparent conversion of Asp-255 or Asp-258 to isoAsp as the ions z_8-57 (diagnostic for isoAsp-255) or z_5-57 (diagnostic for isoAsp-258) were not detected (Figures 2A to 2C). However, following exposure at 37°C for 4 h, the isoAsp diagnostic ETD fragment z_5-57 was detected, indicating isoAsp formation at Asp-258 (see Supplemental Figure 3 online). No z_8-57 ion was detected; thus, no isoAsp formation was found for Asp-255 under these conditions (see Supplemental Figure 3 online). When the protein was incubated at 37°C for 12 h (Figures 2D to 2F), z_5-57 and z_8-57 fragment ions were consistently detected, indicating the formation of isoAsp-258 and isoAsp-255, respectively.

Although the peptides containing isoAsp were not resolved from Asp-containing peptides in these chromatographic conditions, no significant differences in elution pattern were observed irrespective of the temperature of exposure (25 versus 37°C; see Supplemental Figures 4A and 4B online). However, the isoAsp-specific, diagnostic ions were clearly detected by ETD-MS/MS if the protein was exposed to 37°C for 12 h (Figures 2E and 2F), as well as when the protein was subjected to incubation at 45°C, which indicated the formation of isoAsp in the DEAD-box in response to thermal insult. Furthermore, isoAsp diagnostic fragment ions were also observed from Asp-371 when the protein was exposed to 37°C for 12 h yet were absent if the exposure was made at 25°C (see Supplemental Figures 5A and 5B online). This diagnostic ion also was not observed if the protein was exposed to 37°C for 4 h. These results indicate that Asp residues other than those in the DEAD-box region are susceptible to isoAsp conversion upon heat exposure, although it appears likely that the DEAD-box region is more vulnerable to isoAsp formation compared with the other Asp-containing regions of the protein covered in the analysis.

The RNA Helicase Activity of PRH75 Is Compromised by Thermal Stress and Repaired by PIMT

It is apparent that a 4 h, 37°C treatment can convert at least one Asp (in the DEAD-motif) to isoAsp, but are there consequences to catalysis of these conversions? Prior to testing PRH75 helicase activity after heat treatment or the capacity of PIMT to rescue any loss of duplex unwinding activity, it was important to determine the minimum amount of PRH75 required to unwind the RNA substrate under assay conditions of 2 mM ATP and 0.5 nM double-stranded RNA so as to maximize the sensitivity of the PIMT-mediated PRH75 repair assay. Proper interpretation of the unwinding reactions, prior to and after PIMT repair, would be impossible in the presence of excessive amounts of PRH75 because even small percentages of active PRH75 would be indistinguishable from an entirely active population of enzyme when RNA duplex substrate is limiting. Hence, assays were conducted with different concentrations of enzyme and the minimum PRH75 amount, sufficient to unwind maximum RNA duplex at constant duplex and ATP, was determined. This amount of enzyme (0.1 μM) was doubled and used in the assays of PRH75 heat susceptibility and PIMT repair.

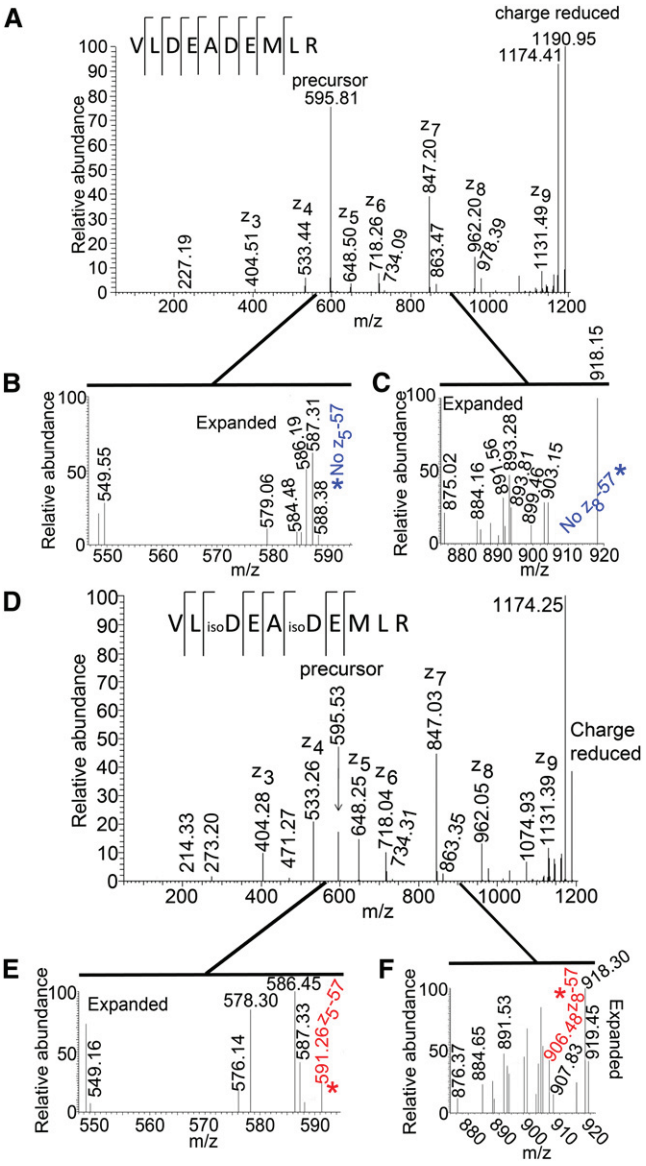

Figure 2. The DEAD-Box Asp Residues Are Susceptible to IsoAsp Formation.

ETD mass spectra of the DEAD-box-associated tryptic peptide VLDEADEMLR (amino acid positions 253 to 262) of PRH75 **(A)**. The tryptic peptide resulting from PRH75 incubated at 25°C for 36 h (expected regions of isoAsp-diagnostic ions z_5-57 for Asp-258 **[B]** and z_8-57 for Asp-255 **[C]** are expanded for clarity) was compared with that from PRH75 **(D)** incubated at 37°C for 12 h with PRH75 incubation preceding digestion with trypsin in both instances. Below the trace in **(D)**, the expected regions of isoAsp-diagnostic ions z_5-57 for Asp-258 **(E)** and z_8-57 for Asp-255 **(F)** are expanded for clarity. The doubly charged precursor ion for the peptide (*m/z* 595.7) was isolated and fragmented by ETD using fluoranthene anions. The observed z-series fragment ions are labeled in the spectra.

[See online article for color version of this figure.]

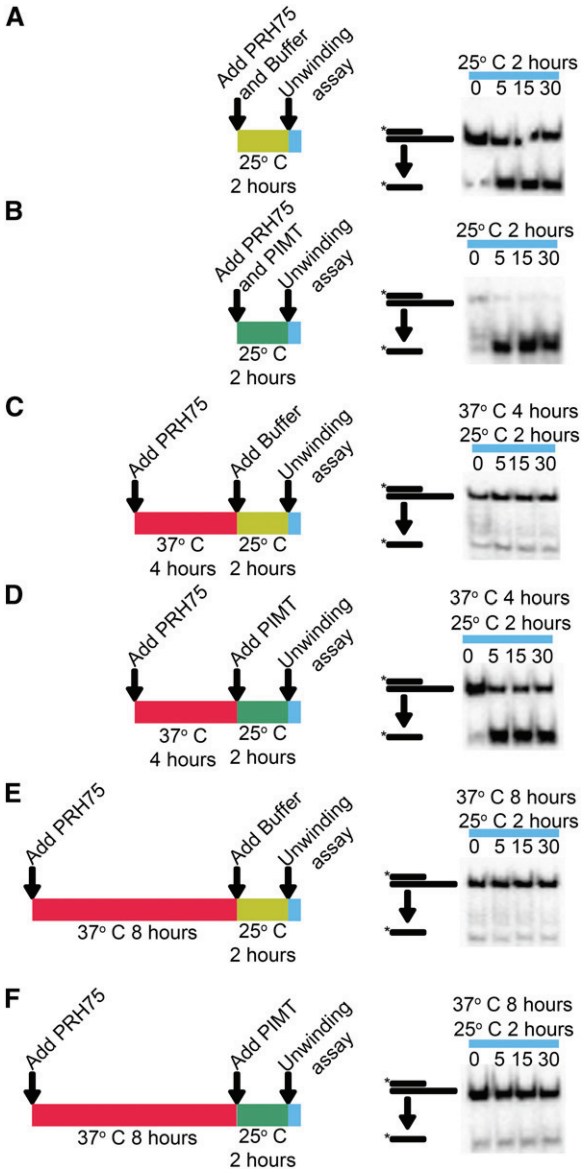

Figure 3. Recombinant PIMT Can Repair PRH75, Recovering Some of the RNA Duplex Unwinding Activity.

A depiction of each assay condition is presented on the left showing PRH75 heat pretreatment, if any (red bar signifying 37°C) prior to buffer or PIMT addition (gold or green bar, respectively) and subsequent incubation at 25°C for 2 h before performing the duplex unwinding assays (light-blue bars). Using 0.2 μM PRH75, the amount of single-stranded product produced over a 30-min period was determined. This quantity was compared for PRH75 that had incubated 120 min at 25°C in the presence of PIMT repair buffer containing AdoMet either without (**[A]**, **[C]**, and **[E]**) or with (**[B]**, **[D]**, and **[F]**) addition of PIMT to a final concentration of 40 μM. PRH75 unwinding activity benefited from PIMT incubation (cf. **[A]** and **[B]**) as did PRH75 thermally insulted for 4 h at 37°C (cf. **[C]** and **[D]**). Heat stress prolonged beyond 4 h prevented subsequent recovery of duplex unwinding activity by PIMT (cf. **[E]** and **[F]**).

To answer this question, we examined unwinding activity after heat treatment and the impact of PIMT on PRH75 activity, before and following the heat treatment. Although PRH75, prior to thermal insult, possessed demonstrable activity without incubation with PIMT, the strand unwinding capacity of recombinant PRH75 benefited greatly from a 120-min incubation with PIMT in the presence of AdoMet, increasing PRH75's capacity to displace RNA duplexes considerably (Figures 3A and 3B). Heating PRH75 to 37°C for as little as 4 h strongly reduced PRH75 activity in the RNA duplex unwinding assay as determined by the static amount of radiolabel present in the short RNA strand relative to that in the duplex over the 30-min assay (Figure 3C). Hence, the PRH75 helicase activity is detrimentally influenced by isoAsp formation (cf. Figures 3A and 3B) and is heat labile (Figure 3C). Incubation with PIMT and AdoMet for 120 min at 25°C, following 4-h thermal insult, partially restored PRH75 RNA duplex unwinding activity (cf. Figures 3C and 3D). These data suggest that inactivation seen after 4-h thermal insult of PRH75 is largely due to isoAsp formation, and repair by PIMT restores the majority of helicase activity.

However, PRH75 enzyme, incubated at 37°C for 8 h, was not amenable to recovery through PIMT-mediated repair (Figures 3E and 3F). This result indicates that longer heat insult leads to further defects in the enzyme which cannot be repaired by PIMT.

The RNA strand rewinding capacity of PRH75 (see Supplemental Figures 2A to 2C online) was more resistant to thermal insult than the duplex unwinding activity (see Supplemental Figures 2D to 2I online). Neither RNA duplex rewinding (see Supplemental Figures 6A to 6C online) nor unwinding (see Supplemental Figures 6D to 6F online) activities, in the absence of PRH75, were influenced by AdoMet and PIMT.

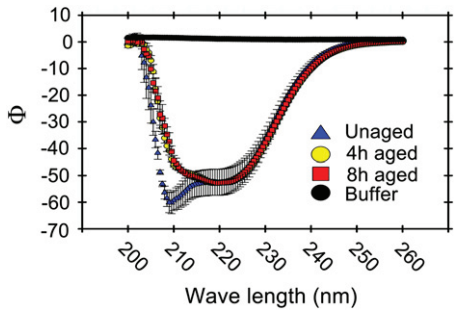

Figure 4. Prior Exposure of PRH75 to 37°C for 4 or 8 h Alters Its Structure.

The average CD spectrum of PRH75 prior to exposure to 37°C (unaged, duplex unwinding capable) exhibited a distinct deflection centered at 209 nm that was absent in spectra of 37°C-treated samples (unwinding incapable; Figure 3). The double deflection at and around this point in the spectrum is typically indicative of proteins containing α-helices (Kelly and Price, 2000). Each point is the average ± SE of CD spectra from three independent protein samples.

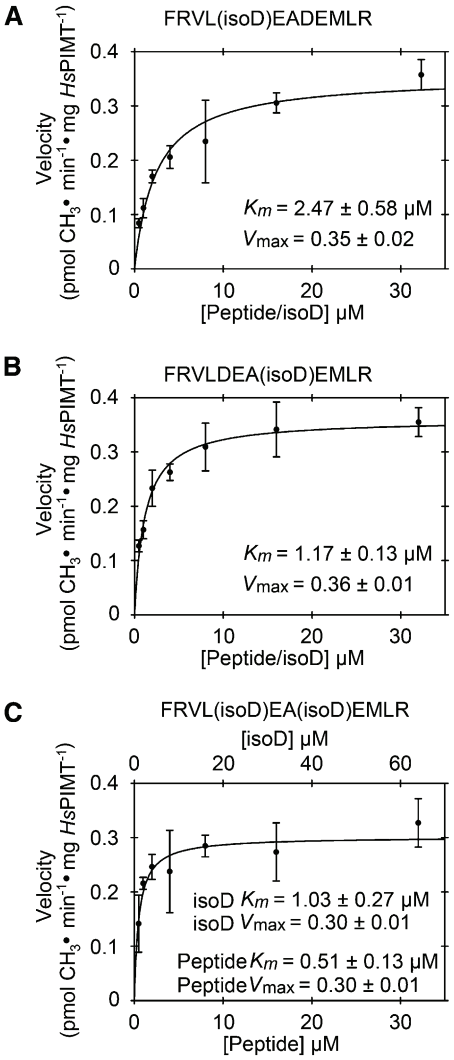

Figure 5. PIMT Can Affect Repair of IsoAsp Residues Separated by as Few as Two Amino Acids Equally as Well as Either Amino Acid Alone.

Enzyme kinetic analysis of PIMT-mediated repair of isoAsp in synthetic peptides of the DEAD-box region of PRH75. Three different peptides, varying in the position at which they had an isoAsp residue, were used as substrates in rPIMT assays to characterize their capacity to partake in the repair reaction. There were two sites in the DEAD-box motif that could potentially convert to isoAsp allowing three different scenarios: the more amino terminal Asp residue converted to isoAsp **(A)**, the more C-terminal Asp residue as isoAsp **(B)**, or both converted to isoAsp **(C)**. For the substrate containing isoAsp at two sites, the V_{max} and K_m have been calculated based on the concentration of peptide (bottom abscissa label) and on the concentration of isoAsp (top abscissa label). Initial velocities for triplicate samples of peptide are expressed relative to the enzyme activity on the methyl-accepting substrate ovalbumin. Each point is the average ± SE from three independent samples for each peptide.

Circular Dichroism–Discernible Structural Change in PRH75 Due to Thermal Insult

It was possible that isoAsp formation in PRH75, leading to the loss of PRH75 activity upon 4-h thermal insult, and/or recalcitrance of PRH75 thermally insulted for >4 h to PIMT repair, was attributable to gross morphological alterations of the enzyme. To test this, circular dichroism (CD) was employed to monitor PRH75 for differences in protein structure brought about by thermal insult. Maximum deflection of the PRH75 CD spectra occurred at 209 nm (Figure 4), one hallmark of the presence of α-helices somewhere in the protein (Kelly and Price,

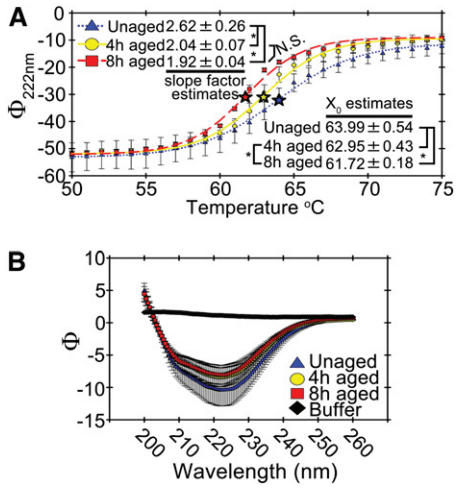

Figure 6. Prior Exposure of PRH75 to 37°C for 4 or 8 h Predisposes the Protein to Denaturation.

To examine the temperature at which half of the PRH75 in a sample denatured, and whether pretreatment at 37°C for 0, 4, or 8 h influenced this profile, PRH75 was thermally scanned by increasing the sample temperature 1°C·min^{-1} from 20 to 85°C, while alterations in the CD signal at 222 nm were monitored. The samples were cooled to 20°C and rescanned (four times for each replication's spectrum) at 25°C using 0.5-nm intervals from 260 to 200 nm, and these scan profiles averaged and standard errors calculated.

(A) The inflection point (X_0; stars) of thermal denaturing curves, estimated from the Boltzmann equation, for PRH75 shifted to lower temperatures upon preexposure to 37°C. Using directional, one-tailed Dunnett's *t* tests (α = 0.05), this deviation was found to be statistically significantly different (asterisk) between unaged PRH75 (greater) and 8 h aged PRH75 (less) but not between unaged and 4-h aged PRH75. The X_0 estimate for 4 h aged PRH75 was also significantly greater than that calculated for 8-h aged PRH75. The estimates for the Boltzmann slope factor for PRH75 after 37°C treatment, regardless of duration, were also statistically significantly different (asterisk) from the unaged control but not between the 4-h aged and 8-h aged protein (N.S., not significant).

(B) Following one round of thermal denaturation to a final temperature of 85°C, and following cooling to 25°C, the CD spectra of PRH75, regardless of prior exposure to 37°C, were of similar shape and attenuated, signifying a considerable loss of dissolved PRH75 due to heat denaturation. All estimates are the average ± SE of Boltzmann equation parameter fits from three independent protein samples. The points on each curve and error bars represent the average ± SE from three independent protein samples.

2000). PRH75 without thermal insult (unaged) was morphologically distinct in the region of the spectra centered at 209 nm from PRH75 heated at 37°C for 4 or 8 h and from the buffer that contained it. However, PRH75 heated for either 4 (repairable) or 8 h (PIMT unrepairable) did not discernibly differ from each other in their CD spectra (Figure 4).

PIMT-Mediated Repair Is Not Sterically Hindered by IsoAsp Residues in Close Proximity

The activity loss of PRH75 exposed to thermal insult for 4 h was partially reversible by PIMT and AdoMet, while the effects of longer heat treatments were not PIMT reversible. Concurrently, 4-h exposure to 37°C resulted in the isomerization of Asp-258, while, after 8 h at 37°C, the additional isomerization of Asp-255 occurred. We hypothesized that while one isoAsp conversion in the DEAD-box may be PIMT reversible, two isoAsp residues in close proximity may hinder effective repair of either. This would succinctly explain the observations of isoAsp occurrence, PRH75 activity loss, PIMT-mediated repair, and subsequent loss of the capacity for PIMT-mediated repair.

To explore the possibility that the failure of PIMT to mediate PRH75 recovery following prolonged incubation at 37°C was due to the formation of isoAsp at both Asp sites in the DEAD-motif, peptides with one or both Asp converted to isoAsp were used as substrates. However, there was no influence of the position of the isoAsp or whether the substrate contained two or one isoAsp, on either K_m or V_{max} when these parameters were calculated based on the concentration of isoAsp in the assays (Figures 5A to 5C), at least in a peptide context.

Prior Thermal Insult Progressively Destabilizes PRH75

None of the isoAsp residues discovered using MS/MS provided a satisfactory explanation of why 4-h heated PRH75 was partially repairable by PIMT while 8-h heated PRH75 was not. Because CD spectra of 4- or 8-h heated PRH75 were similar, we explored the possibility that isoAsp presence led to additional, non-PIMT-repairable, CD spectrum undetectable, protein alterations that would manifest themselves in a less thermally stable PRH75. Thermal denaturation curves described by the Boltzmann equation yielded parameter estimates for both the temperature at which half of the PRH75 was denatured (X_0) and the Boltzmann slope factor (Klassen et al., 2008) that were distinctly and statistically significantly different for PRH75. A progressive decline in the temperature at which half of PRH75 became denatured, in particular, was evident (Figure 6A, Table 1). The difference in PIMT-AdoMet-mediated PRH75 repair between PRH75 thermally insulted for 4 h relative to 8 h indicates that 8-h-exposed PRH75 is the more damaged enzyme. The difference in PRH75 unwinding activity (Figure 3) between untreated PRH75 and 4-h-heated PRH75 defines a clear decline in the catalytic competence of PRH75. These results led us to rank the degree of PRH75 integrity (based on catalysis and repairability) as 0 h > 4 h > 8 h heat-treated enzyme. With this information, a one-tailed Dunnett's t Test was used to compare Boltzmann X_0 estimates between control (0- or 4-h heated PRH75) and these protein's inferior(s) (4- and/or 8-h heat-treated enzyme). The 0 h X_0 was not statistically superior to the 4-h heat-treated protein's X_0 but half of the 8-h-treated PRH75 was denatured at a temperature significantly less than that for untreated PRH75 (Figure 6A). The 8-h estimate was also statistically significantly less than the 4-h estimate for the temperature at which PRH75 is half denatured. The Boltzmann slope factor for PRH75 exposed to 37°C for either 4 or 8 h was significantly different from that of untreated PRH75, but there was no statistically significant difference in the estimates for this parameter between the 4- and 8-h-treated PRH75 (Figure 6A, Table 1). CD spectra of PRH75 following thermal denaturation and subsequent cooling to 25°C could not distinguish among the proteins from the three treatments at 37°C (0-, 4-, or 8-h exposure; Figure 6B).

The drastic reduction in the capacity of the ATP-dependent DEAD-box helicase to effect local strand unwinding after thermal insult for 4 h at 37°C and the recovery of this activity realized following PIMT incubation underlines the dire effect of isoAsp formation on PRH75 enzyme activity in vitro. This prompted an exploration of the consequences of PRH75 dysfunction in vivo.

Table 1. Boltzmann Thermal Denaturing Curve Parameter Estimates for rPRH75 That Had Been Subjected to 37°C for 0, 4, or 8 h

rPRH75 Thermal Denaturing Results		Boltzmann Estimates				
Treatment	Replication/Average	a	Slope Factor (b)	X_0	Y_0	Adj. R^2
0 h 37°C	R1	36.74	3.10	65.01	−43.90	0.999
	R2	44.24	2.23	63.17	−54.15	0.997
	R3	44.96	2.53	63.79	−61.43	0.997
	Average ± SE	41.98 ± 2.63	2.62 ± 0.26	63.99 ± 0.54	-53.16 ± 5.09	0.9985
4 h 37°C	R1	43.18	2.16	62.86	−50.57	0.998
	R2	44.76	1.93	62.25	−53.57	0.998
	R3	39.59	2.03	63.73	−51.88	0.997
	Average ± SE	42.51 ± 1.53	2.04 ± 0.07	62.95 ± 0.43	-51.92 ± 0.79	0.9977
8 h 37°C	R1	43.81	1.99	61.83	−50.67	0.999
	R2	44.18	1.90	61.96	−52.83	0.997
	R3	41.17	1.86	61.36	−52.87	0.998
	Average ± SE	43.05 ± 0.95	1.92 ± 0.04	61.72 ± 0.18	−52.12 ± 0.72	0.9978

Results are presented graphically in Figure 3A.

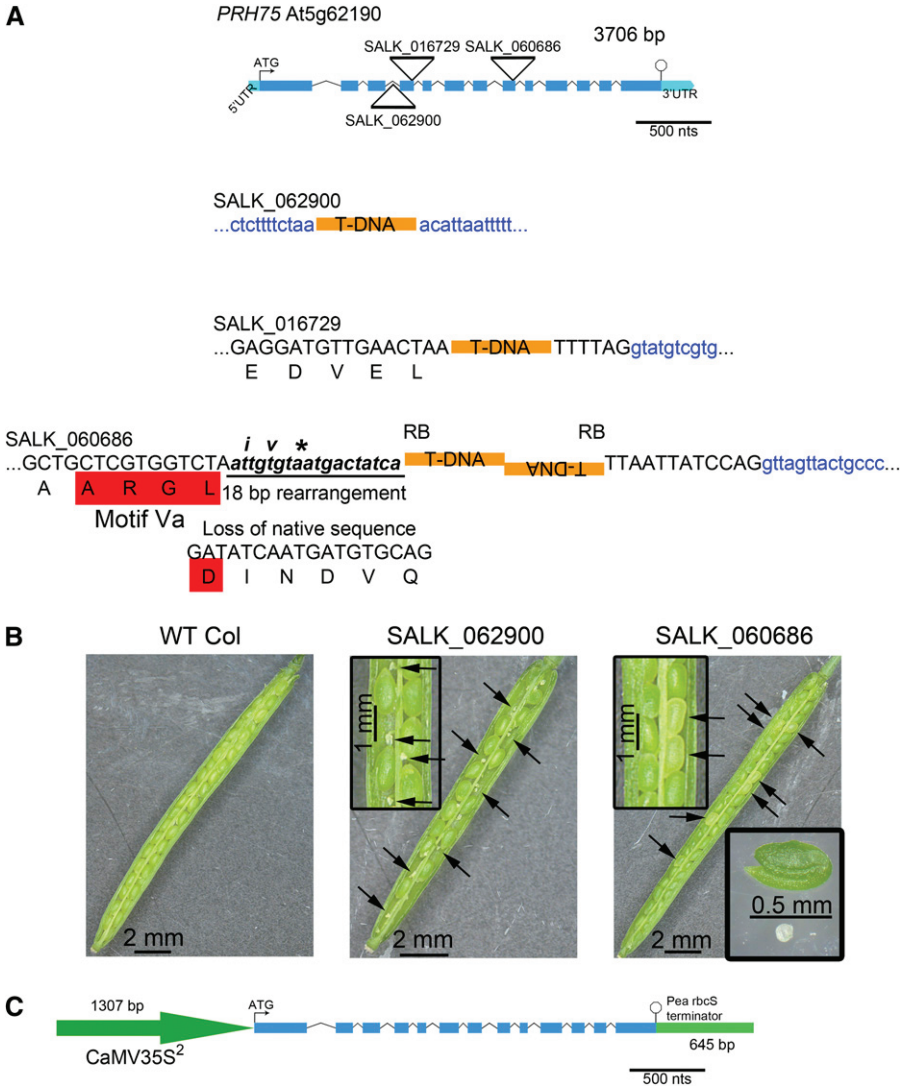

Figure 7. Depiction of the T-DNA Insertion Sites in PRH75 in Lines SALK_062900, SALK_16729, and SALK_060686.

(A) The insertions are located in an intron (SALK_062900) or in exons close to the 5′ end of an intron (SALK_16729 and SALK_060686). The insertion in SALK_060686 results in an 18-bp rearrangement immediately 5′ to the insertion site with a tandem repeat of the T-DNA. This rearrangement (italicized, bold, underlined bases in SALK_060686) results in two new amino acids prior to a premature stop codon (italicized and bold type). nts, nucleotides; UTR, untranslated region.

(B) Immature siliques were removed from wild-type plants or those heterozygous for two of the T-DNA insertions and split with a needle, exposing the seeds within for photography (magnified in the top left insets). One normal appearing and one presumptive homozygous mutant seed from a SALK_060686 plant was dissected and the embryo exposed and photographed (bottom right inset). Black arrows point to some of the presumably aborted ovules or arresting homozygous seeds in siliques. WT, the wild type.

(C) The cassette used to complement the SALK_060686 mutant using the whole gene with the cauliflower 35S mosaic virus promoter driving expression and terminated by the pea (*Pisum sativum*) ribulose-1,5-bisphosphate carboxylase/oxygenase small subunit-E9 polyadenylation site. In all panels, exons are blue rectangles, introns are chevrons connecting the exons, T-DNA insertions are triangles converging on the point of insertion, the 5′- and 3′-untranslated regions are in light blue, and translational start (bent arrow) and stop sites (a white stop sign) are depicted. The DEAD-box motif Va, interrupted by the T-DNA insertion in SALK_060686, is highlighted in red. The cauliflower mosaic virus (CaMV) 35S promoter is a dark-green arrow, and the pea rbcS-E9 polyadenylation site is a green rectangle.

PRH75 Is an Embryo-Defective Gene

Only heterozygotes were recovered for transgenic plants with T-DNA insertions in the gene encoding PRH75, including the SALK_060686, SALK_062900, and SALK_016729 lines (Figures 7A and 7B). Although it had been suggested that the SALK_040581 line carried a T-DNA insert in *PRH75* (Alonso et al., 2003), we were unable to confirm this assignment. The three *prh75* T-DNA insertional mutant lines produced aborted ovules or dead seeds in greater abundance than wild-type

Columbia (Col; Table 2, Figure 7B). Examining siliques of the heterozygous lines, it became evident that seeds of the SALK_060686 line were progressing furthest in development. When developing seeds from siliques from *prh75* heterozygous mutant plants from SALK_060686 were examined after clearing with Hoyer's solution, approximately one-quarter of the seeds per silique terminated embryo development ranging between the globular to torpedo stages (see Supplemental Figures 7A to 7F online; Figure 7B, inset). When transformed with an empty pCAMBIA vector, SALK_060686 plants segregating for both kanamycin (T-DNA) and hygromycin (pCAMBIA) resistance also produced approximately one-quarter dead seeds (Table 2), while kanamycin null segregants appeared similar to wild-type Col. When the SALK_060686 line was transformed with a pCAMBIA vector harboring $35S_{pro}$:*PRH75* (Figure 7C), resulting plants, segregating for both selectable markers (double hemizygous), produced seeds that fit a model where only one in every 16 seeds was dead (Table 2). In subsequent populations of plants selected on kanamycin and hygromycin, it was possible to recover homozygous lines for the T-DNA insert with the complementing transgene that produced as few dead seeds as the wild type.

Eventually, a homozygous *prh75* mutant (from seeds sown on selective Murashige and Skoog media containing Suc) was recovered from the SALK_060686 line, heterozygotes of which produced 25% of their seeds developing furthest prior to abortion and which had the T-DNA insertion site furthest toward the 3′-end of the coding sequence of those T-DNA lines examined (Figure 7A). These plants produced some bolts on which the siliques were frequently undeveloped, relative to the wild type (Figures 8A and 8B). However, the plants also produced siliques of normal appearance on the same bolt (Figure 8B, arrows). Seeds from *prh75* were varied in appearance, relative to the wild type, ranging from seemingly wild-type to oddly shaped, shrunken seeds that were, nonetheless, viable (Figures 8D, 8E, 8G, 8H, 8J, and 8K). The undeveloped siliques and oddly shaped seeds were obviated in *prh75* $35S_{pro}$:*PRH75* plants (Figures 8C, 8F, 8I, and 8L).

DISCUSSION

Arabidopsis PRH75 Unwinding Activity Is Compromised by IsoAsp Formation

In this work, we have shown that the DEAD-box helicase PRH75 possesses unwinding activity. This activity is lost after 4-h thermal insult, but it can be recovered by PIMT and AdoMet. This result suggests that formation of isoAsp contributes to this activity loss and that isoAsp repair by PIMT can restore activity. The stability of the duplex in assays where PIMT was added to PRH75 thermally insulted for more than 4 h indicates that prior apparent PRH75 activity enhancement (no thermal insult; Figure 3B) or partial recovery (4 h; Figure 3D) was not due to introduction of contaminating helicase activity from *Escherichia coli* from which the PIMT was purified (see Supplemental Figures 6A to 6F online) but instead constitutes bona fide PRH75 repair by PIMT. The rapidity of the onset of enzyme dysfunction and the drastic reduction in duplex unwound (cf. Figures 3A and 3C) suggest that isoAsp formation may be one of the initial, debilitating forms of protein damage assailing heat-shocked PRH75. The relative insensitivity of the strand annealing activity to thermal insult indicates that the PIMT-repairable isoAsp(s) does not affect this activity.

Where in PRH75 Does IsoAsp Formation Occur?

If isoAsp formation directly interfered with catalysis, only two motifs are susceptible. PRH75 motif II (Asp-255 and Asp-258, the DEAD-box) and motif Va (Asp-411) are the only motifs (from Q through VI) containing Asx residues (see Supplemental Figure 1A online); however, we found a considerable improvement of PRH75 activity, prior to thermal insult, by incubation with PIMT. There was no isoAsp detectable in PRH75 at this time over the portion of the protein monitored using LC-MS/MS. Hence, the early loss of some of the helicase activity (prior to heat shock) cannot be a direct consequence of Asp-255 or Asp-258 isoAsp conversion (motif II). Furthermore, it is unlikely that the enzyme could bind to both ATP and RNA duplex but fail to hydrolyze the

Table 2. χ^2 Analysis (One Degree of Freedom) of a Goodness of Fit to Various Genotypic Ratios Based on the Hypothesis That Homozygous *prh75* Insertional Mutants Were Embryo Defective

Category	Wild Type	SALK_ 016729	Wild-Type Sib	SALK_ 060686	Wild-Type Sib	SALK_060686			
	–	Het	–	Het	–	Het1 MT Vector	Het1 35S $_{pro}$:*PRH75* s	Het2 MT Vector	Het2 35S $_{pro}$:*PRH75* s
Dead seeds	13	276	27	355	13	323	70	297	64
Live seeds	1128	857	1122	1115	1116	943	1038	955	1015
Total seeds	1141	1133	1149	1470	1129	1266	1108	1252	1079
Model	3:1	3:1	3:1	3:1	3:1/15:1	3:1	15:1	3:1	15:1
χ^2	346	0.247	314	0.567	342/50	0.178	0.009	1.091	0.187
Dev. from model	Sig.		Sig.	ns	Sig./Sig.	ns	ns	ns	ns

Data from wild-type Col, two different alleles heterozygous for the insertion, and their wild-type sibs are provided. One of the heterozygous mutants was complemented with an empty vector (MT) or with the cauliflower mosaic virus 35S promoter ($35S_{pro}$) driving constitutive expression of the *PRH75* gene. In the heterozygous plants, the lower case "s" following the $35S_{pro}$:*PRH75* designates lines segregating for the complementing construct. Het, heterozygous; Dev. from model, significant deviation from the proposed model based on χ^2 analysis; Sig., significant deviation; ns, no significant deviation.

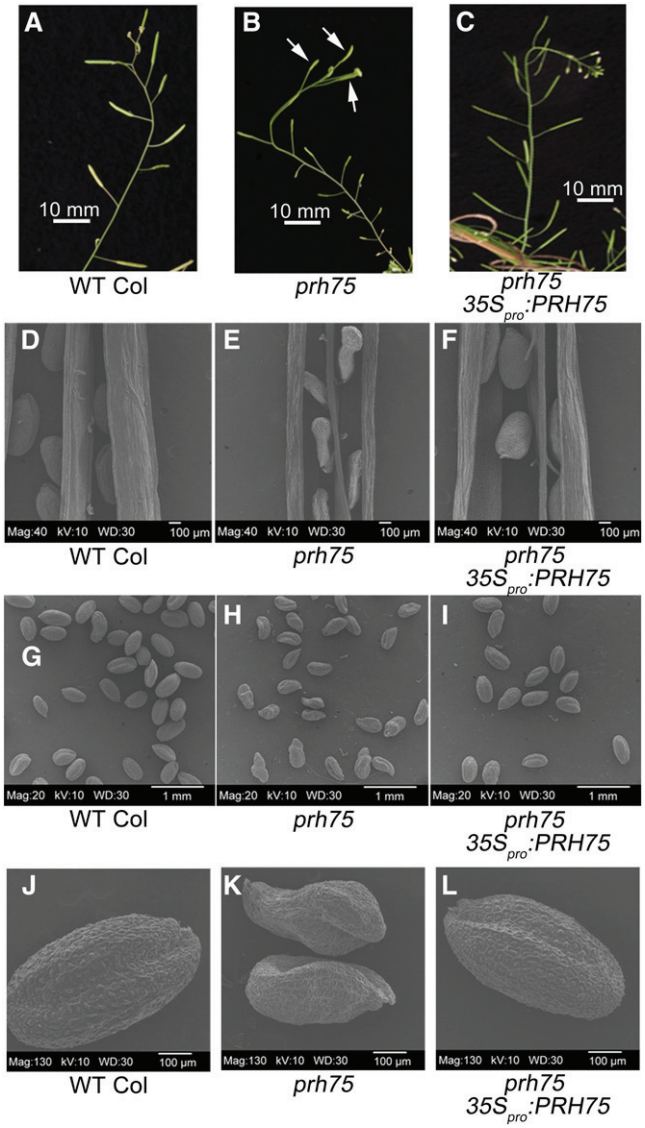

Figure 8. The *prh75* Mutant Produces Small Siliques Containing Seeds Altered in Shape.

(A) to **(C)** The *prh75* mutant bolt develops a variety of silique sizes, relative to the wild type (WT) or 35S$_{pro}$:*PRH75* complemented *prh75*. While some are small, others (arrows) are similar to the wild type in appearance.
(D) to **(F)** Some of the *prh75* siliques contain seeds of altered morphology compared with the wild type or complemented *prh75*.
(G) to **(L)** However, not all *prh75* seeds are distinctly different from wild-type or complemented *prh75* seeds.
[See online article for color version of this figure.]

former (thereby releasing the latter) because this would not influence strand disassociation (it would still occur), resulting in the loss of the radiolabeled strand from the enzyme/RNA complex. Both enzyme and ATP are in excess of RNA duplex in these single-cycle reactions. This observation renders the possibility that a loss of helicase activity is a direct consequence of Asp-411 isoAsp conversion (present in unmonitored motif Va) unlikely because it is associated with the coordination between RNA binding and ATP hydrolysis (Jankowsky and Fairman, 2007).

The enzyme activity lost in the recombinant PRH75 prior to heat shock and recovered by incubation with PIMT and AdoMet must be a consequence of isoAsp formation throughout the protein or at a hot spot unmonitored in this LC-MS/MS analysis that lies between the motifs required for duplex unwinding. In a typical LC-MS/MS experiment, there were ~17 unmonitored Asx sites between the Q and the VI motifs, any one of which might be highly susceptible to isoAsp formation and potentially responsible for the rapid loss of enzymatic function. Due to the necessity of stringently purifying RNA-modifying enzymes if they are to be assayed against their degradation-prone substrate, some isoAsp may be introduced into the protein being purified if it is susceptible to this alteration. The in vitro introduction of isoAsp into protein during purification and/or storage prior to analysis has been reported previously (Yang and Zubarev, 2010). While these two eventualities cannot currently be resolved, it is obvious that PRH75 activity is highly susceptible to isoAsp formation, which negatively influences RNA unwinding.

It is our contention that the introduction of an extra carbon atom in the PRH75 peptide backbone (through isoAsp formation at a site between motifs) is sufficient to alter protein secondary structure and misalign amino acids whose three-dimensional coordination is crucial for substrate binding and catalysis. This is particularly relevant for DEAD-box RNA helicases, whose two RecA-like helicase motifs are tethered to each other by a flexible linker and undergo substantial realignment about this anchor upon ATP binding (Jankowsky and Fairman, 2007). Repair of these isoAsp residues as they arise, or shortly thereafter, might allow the protein to realign and recover some or all of its activity.

The ensuing loss of the capacity to recover PRH75 activity following PIMT-mediated repair when thermal insult was prolonged beyond 4 h was intriguing as additional, non-PIMT-repairable alterations to PRH75 secondary structure must occur. However, there are no gross morphological alterations that occur in PRH75 between the 4- and 8-h thermal insult evident using CD; rather, more subtle alterations occur that render PRH75 incubated at 37°C for 8 h more susceptible to thermal denaturation following additional heat treatment (thermal

Table 3. Primers Used in This Study

Possible Insertion	Primers
SALK_040581	F 5′-ATCTCTCAACAAGCAGAAGAG-3′
	R 5′-ATACCTGACCAGTACGAGCCC-3′
SALK_016729	F 5′-TCGGTATTGTGAATCTCCTGC-3′
	R 5′-CATGGCTGCCTTATTACAAGG-3′
SALK_062900	F 5′-TTGGGTTTTGCTTATTATGCG-3′
	R 5′-AGAAGCAAGCGAAAAGGTCTC-3′
SALK_060686	F 5′-TCACTATCTAGTGGAGGCCAAAC-3′
	R 5′-TTTTCGTAAGACAAACCGCAG-3′
LBb1.3	5′-ATTTTGCCGATTTCGGAAC-3′
Right border	5′-GCGGTTCTGTCAGTTCCAAACG-3′
PRH75 for pET	F 5′-CATATGCCTTCCCTAATGTTATCTGATAAG-3′
PRH75 for pET	R 5′-CTCGAGATATCTCTGGCCTCTACCACC-3′

F, forward; R, reverse.

scanning). This continuum of damage to PRH75 is visible in the progressive trend to the left along the abscissa of the PRH75 thermal denaturation curves (Figure 6A). PRH75 has been reported to physically interact with at least two peptidyl-prolyl *cis-trans* isomerases (GeneMANIA; Razick et al., 2008; Warde-Farley et al., 2010) responsible for altering the relative orientation of Pro and its N-terminal neighbor in the protein backbone (Galat, 1993). Nonenzymatic Pro isomerization is known to occur slowly, overcoming a considerable energy barrier (Chen et al., 2012), although this process accelerates with increasing temperature (Kern et al., 1997), resulting in deleterious consequences for enzymatic activity, should it not be rectified (Cloos and Christgau, 2002; Wedemeyer et al., 2002). It is possible that peptidyl-prolyl *cis-trans* isomerase association with PRH75 underlies a propensity for the helicase to also undergo Pro isomerization and deactivation over time, a subtle protein alteration that PIMT would be incapable of reversing. It is certainly noteworthy that, for whatever the reason, the apparent efficiency of strand separation and enzyme substrate(s) affinity of at least this DEAD-box RNA helicase can be profoundly influenced by the presence of isoAsp somewhere in the protein.

PRH75 Is an Essential Enzyme for the *Arabidopsis* Life Cycle

PRH75 is a so-called *embryo defective* (*emb*) gene, essential for the production of a viable sporophyte (Meinke et al., 2008). Despite the fact that there are at least 58 DEAD-box helicases present in the *Arabidopsis* genome (Mingam et al., 2004), apparently none shared sufficient redundancy with PRH75 given the lethality of the *prh75* mutation. There have been 800 *emb* genes identified to date in this model plant, of which seven were D/RNA helicases (At1G01040, At1G08840, At1G12770, At1G20960, At1G32490, At3G53110, and At5G26742) (Tzafrir et al., 2004), and an additional four D/RNA helicases, other than PRH75, have since been identified as belonging to the *emb* category (At1G70070 [Kobayashi et al., 2007], At2G35340 [Pagnussat et al., 2005], At5G08610 [PIGMENT DEFECTIVE 340 SeedGenes database], and At5G13010, FREYA [Johnston et al., 2007]). One D/RNA helicase is known to result in embryo sac developmental arrest (At1G61140, EMBRYO SAC DEVELOPMENTAL ARREST16) prior to fertilization (Pagnussat et al., 2005). Conservatively, 1.5% (12/800) of these essential genes encode D/RNA helicases.

PRH75 encodes an essential enzyme, which emphasizes that the consequences for cellular homeostasis of widespread PRH75 dysfunction are catastrophic unless a means of repairing or replacing the enzyme exists. An enzyme can be replaced through de novo transcription (Li et al., 2001) assuming the whole of the translational apparatus is intact and functional. While this is usually the case, nowhere in the plant is this generalization more jeopardized than in cells of dehydrated seeds (Kushwaha et al., 2013), where spontaneous succinimide formation (the first step in isoAsp formation) but not protein repair is possible in the anhydrous environment (Desfougères et al., 2011). Upon imbibition (rehydration), succinimide rapidly and spontaneously hydrolyzes to either Asp (~15 to 30%) or isoAsp (~85 to 70%). Hence, as much as 85% of the strand disassociating activity of PRH75 could be inactivated in this manner early during seed germination. If PRH75 can be used as a paradigm, the ubiquity of at least one Asp residue in motif II in enzymes comprising superfamily II (Fairman-Williams et al., 2010), and the susceptibility of Asx residues at this and other sites in PRH75 to isoAsp formation makes it possible that this class of enzyme is a prime PIMT target in a host of organisms. General (superfamily II helicases) and inclusive (most molecules of each type of helicase) dysfunction due to isoAsp formation would inhibit transcription and leave stored and de novo–synthesized RNA in the cell predominantly in a duplexed form with consequences for splicing, nuclear egress, and translation. Only after sufficient repair of isoAsp in helicases had occurred could these events proceed normally, assuming that isoAsp formation did not lead to additional, non-PIMT-repairable damage. It has been suggested that the ATP/ADP ratio dictates the efficiency with which RNA duplexes are unwound in vivo (Yang and Jankowsky, 2005). An additional degree of complexity would be introduced in dehydrated, quiescent, or dormant seeds when, upon imbibition, a substantial fraction of all DEAD-box helicase proteins in a cell simultaneously suffers isoAsp formation, detrimentally affecting their activity. This may be one reason why the longevity of PIMT-deficient seeds is compromised (Ogé et al., 2008; Verma et al., 2013).

METHODS

Recombinant Protein Production and Purification

The human PIMT coding sequence from plasmid pDM2x (MacLaren and Clarke, 1995) was subcloned into pET30b (Novagen) in frame with an N-terminal hexahistidyl tag. Best expression was from fresh transformations into BL21(DE3)RIL cells (Stratagene) and maximum recovery of soluble protein was with growth in Luria-Bertani medium with appropriate antibiotics at 37°C to an OD_{600} of 0.6 before IPTG induction (50 μM with respect to IPTG). Upon induction, cells were shifted to 22°C and harvested 8 h later. The human PIMT was used in all experiments due to its high affinity for L-isoaspartyl substrates (Chen et al., 2010).

The coding sequence of PRH75 (At5g62190) was amplified from RT-RNA from mature, dehydrated *Arabidopsis thaliana* cv Col seeds and cloned into pET23b (Novagen), and recombinant protein production commenced on each occasion by the fresh introduction of the plasmid described above into *Escherichia coli* strain BL21(DE3)RIL. Five-milliliter starter cultures were added to two 1-liter cultures and grown (OD_{600} = 0.7) until induced (isopropyl β-D-1-thiogalactopyranoside – IPTG – to 0.1 mM) and shifted to 25°C. Cells were harvested 4.5 h thereafter.

For both PIMT and PRH75, recombinant protein was first recovered in lysates (50 mM Tris-HCl, pH 7.5, 500 mM NaCl, 1mM PMSF, 5 $\mu g \cdot mL^{-1}$ pepstatin-A, and 10 $\mu g \cdot mL^{-1}$ leupeptin) from sonication (output 8, 60% duty, 10 min, in a brine/ice bath). Following centrifugation and filtration (0.45-μm polyethersulfone membrane; Sarstedt), lysate was introduced onto a 1.0-mL, nickel-charged, GE HiTrap Ni-agarose column. The column was washed using a gradual introduction of imidazole to 157.5 mM. The column was then flushed with aliquots of 1.0 M imidazole. Aliquots with the greatest recombinant protein amount were combined. At this stage, PIMT was sufficiently pure for use and, following dialysis to remove the imidazole, it was concentrated (10YM Centricon filters; Amicon), protein amounts were ascertained (Lowry et al., 1951; DC Protein Assay; Bio-RAD), and aliquots were flash frozen in liquid N_2 and stored at −80°C. Depending on the final use (CD or helicase activity assay), PRH75 was dialyzed against 20 mM potassium phosphate buffer, pH 7.7, and 50 mM $(NH_4)_2SO_4$ (suitable for CD analysis; Kelly et al., 2005) or underwent

additional purification (helicase assay; see below). The PRH75 for use with CD was retrieved from dialysis, the protein amounts were ascertained (Lowry et al., 1951; DC Protein Assay), and aliquots (200 µL) were snap frozen in liquid N_2 before being stored at −80°C.

For additional purification, fractions of PRH75 recovered from the 1 M imidazole aliquots were diluted 1/10 with 1× ZBf (1× ZBf is 50 mM Tris-HCl, pH 8.0, 2 mM DTT, 1.0 mM EDTA, 50% [v/v] glycerol, and 0.10% [v/v] Triton-X 100). This was mixed with Phospho-cellulose P11 beads (PhosCel; Whatman) prepared from a 50 mL stock of beads, primed according to the manufacturer's instructions, and preequilibrated 12 h in 25 mL 1× ZBf at 4°C. The bead/protein slurry was mixed 2 h at 4°C before being poured into a column (Bio-Rad). The Phospho-cellulose bed was washed with 20 mL 1× ZBf containing 100 mM NaCl and then with 20 mL 1× ZBf containing 200 mM NaCl at flow rates of 0.1 $mL \cdot s^{-1}$. PRH75 was eluted from the Phospho-cellulose bed with 1× ZBf containing 500 mM NaCl at a flow rate of 0.4 $mL \times min^{-1}$, collected in 1-mL fractions. Fractions containing PRH75 were combined, concentrated (10YM Centricon filters), the protein amount ascertained (Lowry et al., 1951; DC Protein Assay), and aliquots (10 µL) frozen on dry ice 2 h before being stored at −80°C.

Helicase Assay

Substrate Preparation

RNA substrates were designed according to the rationale by Rogers et al. (1999) with the 10-nucleotide RNA 5′ end labeled as described by Jankowsky and Putnam (2010). Following incubation for 1 h at 37°C, 2 µL of 5× denaturing gel loading buffer (80% formamide, 0.1% bromophenol blue, and 0.1% xylene cyanol) was added to the labeled RNA. The reaction was heated for 2 min at 95°C and was loaded onto a 20% polyacrylamide denaturing gel and run for 2 h at 30 $V \cdot cm^{-1}$ of gel length, disassembled, wrapped in plastic wrap, and exposed briefly to film to localize the radiolabel. The 10-nucleotide RNA was cut from the gel and eluted overnight at 4°C in 600 µL of RNA elution buffer (300 mM NaOAc, 1 mM EDTA, and 0.5% SDS). Following elution, the gel slice was centrifuged and the supernatant recovered. RNA was precipitated in 3× volume of 100% ethanol with 2 µL of 50% glycerol, placed on dry ice for 1 h, and then centrifuged (16,000*g*) for 30 min at 4°C. The supernatant was removed and the pellet was dried in a SpeedVac for 15 min. The RNA was resuspended in 16 µL of water, 2 µL of duplex annealing buffer (100 mM MOPS, pH 6.5, 10 mM EDTA, and 0.5 M KCl), and 2 µL 100 µM unlabeled 35-nucleotide complementary RNA. The solution was heated to 95°C for 2 min and gradually brought to room temperature over a period of 1 h. After attaining room temperature, 4 µL of 5× nondenaturing gel loading buffer (50% glycerol, 0.1% bromophenol blue, and 0.1% xylene cyanol) was added and the reaction was loaded onto a nondenaturing 15% polyacrylamide gel (0.8 mm thick) prerun for 30 min. The gel was run (~20 $V \cdot cm^{-1}$ gel length) for 2 h. Purification from the gel and duplexed RNA recovery was as described above. The pelleted duplex RNA was dissolved in RNase-free water. The concentration of the labeled duplex was measured by a scintillation counter.

Unwinding and Rewinding Conditions

Both reactions were performed as described by Yang and Jankowsky (2005).

PRH75 Characterization

Assays were run without PRH75 or without ATP to establish the stability of the RNA duplex substrate. Next, ATP amounts were held at 2.0 mM, and duplex RNA substrate concentrations were 0.5 nM throughout, but PRH75 amounts were altered (0.01, 0.025, 0.05, 0.1, 0.25, 0.5, and 1.0 µM). The assays were sampled at five time points over a 1-min reaction time course and were finally measured again at 15 min. The 0.01 and 0.025 µM enzyme concentrations were also sampled at 5 min.

Assay of the Capacity for PIMT to Rescue PRH75 Activity

To enhance the sensitivity of the PRH75 RNA unwinding assay to repair by PIMT, the minimum amount of PRH75 required to arrive at a consistent proportion of duplex unwound (i.e., further increases in enzyme amounts in the assay did not result in any further increase in the proportion of duplex unwound) was documented from the characterization above, and this amount was doubled in the assays used to ascertain the ability of PIMT to repair PRH75.

The PIMT repair of PRH75 experiments subjected PRH75 to 37°C for 0, 4, 8, 12, 24, 72, or 96 h, and these PRH75 samples then received 10 µM AdoMet and were held at 25°C for 120 min. However, only one aliquot was supplemented with PIMT to 40 µM final concentration before the 120-min incubation, the other receiving only buffer. Unwinding activity was then tested at various times over a 30-min time span for each aliquot of the thermally insulted helicase that had or had not been incubated with PIMT. In the experiments, the final PRH75 enzyme concentration was 0.2 µM, with 0.5 nM RNA duplex, and 2 mM Mg-ATP.

CD Spectra and Thermal Scans of PRH75 before and after Thermal Insult

Three replications of samples thermally insulted (37°C) for 0, 4, or 8 h were examined using CD (Jasco J-810 spectropolarimeter) from 260 to 200 nm (decreasing by 0.5-nm intervals) at 25°C (four scans for each replication's spectrum) and the replicate spectra averaged and standard error calculated. These samples were next thermally scanned at 222 nm as the sample temperature was raised 1°C · min^{-1} from 20 to 85°C. The samples were cooled to 20°C and rescanned (four times for each replication's spectrum) at 25°C using 0.5-nm intervals from 260 to 200 nm, and these scan profiles averaged and standard errors calculated. Average CD spectra for buffer and buffer containing PRH75 protein thermally insulted for 0, 4, or 8 h were overlaid using Sigma Plot version 12 (Systat Software). Similarly, sigmoidal curves were fitted to the thermal denaturing data for each replication using the Analysis function of Sigma Plot with a dynamic fit to the Boltzmann equation compiled as by Brown (2001). The parameter estimates defining each replication's thermal denaturing curve were used as independent estimates to determine if the thermally insulted proteins differed significantly from each other in their thermal stability (see Statistical Analysis below).

Investigation of IsoAsp Formation in PRH75 by LC-MS/MS

Sample Preparation for MS

Ten micrograms of purified PRH75 (1 µg · $µL^{-1}$) was exposed to 25 or 37°C for different time intervals. Approximately 2.5 µg equivalent of protein was withdrawn after 4, 12, 24, and 36 h of exposure and precipitated with cold acetone overnight at ×20°C. The precipitate, after centrifugation (12,000*g* for 15 min) and washing with 70% acetone, was resuspended in 10 µL of 6 M guanidine-HCl (Sigma-Aldrich) and 50 mM Tris-HCl, pH 7.9. The protein was subsequently treated with DTT (22 mM) for 30 min followed by iodoacetamide (Sigma-Aldrich) (55 mM) in the dark for another 30 min at room temperature. The sample was diluted with 50 mM NH_4HCO_3 (to obtain <1 M guanidine-HCl final concentration) and digested with trypsin (0.2 µg; Promega) at 25°C overnight. The tryptic peptides were purified by C-18 ZipTips (Millipore) as per the manufacturer's instructions and analyzed by LC-MS/MS.

LC-MS/MS

LC-MS/MS analysis was performed on an LTQ-XL linear ion trap mass spectrometer (Thermo Fisher) equipped with an electrospray ionization source and an ETD source with fluoranthene as the ETD reagent. Tryptic peptides were separated using a Thermo Surveyor HPLC system on an Xbridge C18 1.0 × 150-mm column (Waters) at room temperature using mobile phase A (95% water, 5% CH_3CN, and 0.1% formic acid) and B (95% CH_3CN, 5% water, and 0.1% formic acid). The gradient consists of (1) 5 min at 5% B for sample loading, (2) linear from 5 to 50% B in 55 min, (3) linear from 50 to 80% B in 3 min, and (4) isocratic at 80% B for 12 min before reequilibration. The flow rate was maintained at 70 $\mu L \cdot min^{-1}$. Mass spectra were recorded in positive polarity at a capillary temperature of 275°C, spray voltage of 4.5 kV, and sheath gas, auxiliary gas, and sweep gas set to 35, 10, and 15 arbitrary units, respectively. ETD-MS/MS (normalized collision energy 35%) was used in data-dependent mode to switch automatically between the MS scan (mass-to-charge ratio [*m/z*] range of 365 to 2000 in zoom scan or enhanced scan mode) and three sequential ETD-MS/MS scans of the most abundant precursor ions (two *m/z* unit isolation width). Each ion selected for ETD was analyzed for up to 30 s or 50 scans before it was added to a dynamic exclusion list for 30 s. The chemical ionization source parameters for fluoranthene were optimized as per the standard operating procedure. The duration time of ion/ion reactions was optimized for doubly charged ions, with a supplemental activation function integrated into the ETD data acquisition method. Multiply charged precursor ions were selected for acquisition of targeted tandem mass spectra to monitor the levels of the c_n and $z_{(l-n)+1}$ ion series' and isoAsp-specific reporter ions c_n +57 and $z_{(l-n)+1}$ −57, where *n* is the position of Asp/isoAsp from the N terminus and *l* is the total number of amino acids in the peptide (O'Connor et al., 2006; Yang and Zubarev, 2010).

Recognition and Repair of Synthetic Peptides Derived from PRH75 by PIMT

Three dodecapeptides were synthesized by Biomatik based on the amino acid sequence surrounding the PRH75 DEAD-box (FRVLDEADEMLR) but with the first, second, or both Asp residues replaced with isoAsp. These peptides were then tested as substrates of the human rPIMT. Initial velocities of the methylation reaction were measured at different peptide concentrations in an assay containing rPIMT (0.35 pmol methyl groups transferred $\cdot min^{-1}$) in a final volume of 40 μL of 0.1 M bis(2-hydroxyethyl)-amino-tris(hydroxymethyl)methane chloride at pH 6.4 and 10 μM *S*-adenosyl-[methyl-^{14}C]-L-Met (Perkin-Elmer; 124 dpm $\cdot$ pmol^{-1}). Reactions were conducted according to published protocol (Lowenson and Clarke, 1991). Ovalbumin (Sigma-Aldrich chicken egg white albumin, Grade V) was used as a control substrate at a final concentration of 0.63 mM.

Analysis and Complementation of T-DNA Insertional Mutants of *PRH75*

Four independent T-DNA interrupted mutants for *PRH75* (SALK_062900, SALK_016729, SALK_060686, and SALK_040581) were identified (Alonso et al., 2003), and seeds were acquired from the ABRC (Ohio State University, Columbus, OH). Genomic DNA was isolated for each of these alleles from leaf disks using Extract-N-Amp (Sigma-Aldrich). DNA was amplified using RedTAQ (Sigma-Aldrich) in PCRs using a PE GeneAmp 2400 thermocycler with gene-specific primers (Table 3) on either side of the insertion site (SIGnAL iSECT tool) or one gene-specific primer and an outward facing primer in the T-DNA for both right and left borders. Reactions were initiated at 95°C for 3 min followed by 40 cycles of 95°C for 1 min, 60°C for 1 min, 72°C for 2 min, and a 10-min, 72°C final elongation. Amplicons were isolated and sequenced (BigDye Terminator v3.1 cycle sequencing kit; Applied Biosystems) to identify the exact insertion sites and flanking regions.

Heterozygous plants of the SALK_060686 line, the least deleterious mutant based on the placement of the T-DNA insertion most proximal to the 3′ end of the coding sequence (selected because this line exhibited kanamycin resistance), were exposed, using floral dip (Clough and Bent, 1998), to *Agrobacterium tumefaciens* GV3850 harboring a construct residing in pCAMBIA1301 consisting of $35S_{pro}$:*PRH75*. To acquire empty vector negative controls, the pCAMBIA1301 vector with the empty $35S_{pro}$:MT and rbcS terminator was transformed into heterozygotes of the SALK_060686 line. Seeds from T0 plants were surface sterilized and sown on selective Murashige and Skoog media with 3% Suc and 50 $\mu g \cdot mL^{-1}$ hygromycin and resistant plants obtained. These transformants were transferred to Metromix 200 (Scotts) and the seeds from them tested for segregating kanamycin and hygromycin resistance. For each line (the empty vector or the complementing transgene), doubly resistant plants were transferred to soil and tested using PCR for T-DNA disruption of one of both *PRH75* homologous pairs.

Determination of Embryo Lethality and Complementation

For all genotypes, embryo lethality data were recorded according to Meinke (1994). Seeds from single green siliques from heterozygous plants were dissected and photographed or were placed in Hoyer's solution (Schwartz et al., 1994; Wang et al., 2004) up to 24 h (depending on the age of the seed) before each was photographed using differential interference contrast using an Axioplan2 microscope (Carl Zeiss) to attempt to determine the maturity stage at which the mutant embryos arrested during development.

Recovery of a *prh75* Mutant

The insertional mutant terminating embryo development latest (SALK_060686) was repeatedly screened on Murashige and Skoog medium, 4% Suc, and 100 μM kanamycin plates. Eventually, a kanamycin-resistant, slow-growing seedling screened positive using PCR for a homozygous insertion in *PRH75*. Homozygosity was confirmed in the next generation by 100% survival on kanamycin.

Seedlings of *prh75*, wild-type Col, and $35S_{pro}$:*PRH75* complemented *prh75* were grown and siliques on bolts photographed. Mature, dehydrated seeds, or partially opened siliques from the above plants were fastened to aluminum stubs and sputter coated with palladium:gold (Hummer VI; Anatech) prior to observation using a scanning electron microscope (S-800 scanning electron microscope; Hitachi High Technologies America), and images were captured using Evex Nano Analysis digital imaging system.

Statistical Analysis

Independent parameter estimates of Boltzmann curves describing thermal denaturing profiles of PRH75 after 0, 4, or 8 h prior exposure to 37°C for each replication were used in an analysis of variance to determine if the parameters were statistically significantly different. Because it was known that the integrity of PRH75, based on catalytic capacity loss due to aging, and the loss of PRH75 repair between 4- and 8-h heat treatment, was progressively compromised, a directional (0 h > 4 h> 8 h), one-tailed Dunnett's t Test (α = 0.05) was used to ascertain treatment differences following analysis of variance. For this test, depending on the comparison, Boltzmann parameter estimates for either 0-h heat-treated or 4-h heat-treated PRH75 were used as the control and compared with 4-h- or 8 h-treated or 8-h-treated PRH75 estimates, respectively.

Embryo lethality data were entered into SAS and tested using χ^2 for a goodness of fit to a 1:3 dead:live seed ratio expected for a recessive, lethal mutation, and a random distribution of dead seeds within the pedicelar and stigmatic halves of a silique. The same was done with

wild-type controls grown at the same time, on the same shelf, to ensure that cultural conditions were not contributing to the phenotype. A similar analysis was performed on siliques from double heterozygous plants (T-DNA and complementing, $35S_{pro}$:*PRH75* transgene versus T-DNA and empty vector control), and calculations were performed to assess a 15:1 live:dead seed ratio. Assessments of the number of dead seeds found in siliques from homozygous lines of *prh75* $35S_{pro}$:*PRH75* were also conducted.

Accession Numbers

Sequence data from this article can be found in the GenBank/EMBL libraries under accession numbers At5g62190 (PRH75) and NM_001252053 (PIMT).

Supplemental Data

The following materials are available in the online version of this article.

Supplemental Figure 1. Typical LC-ETD-MS/MS Analysis of Tryptic Peptides of PRH75.

Supplemental Figure 2. Recombinant PRH75 Possesses a Robust RNA Rewinding Capacity.

Supplemental Figure 3. The Aspartates of the DEAD-Box Are Differentially Susceptible to IsoAsp Formation.

Supplemental Figure 4. IsoAsp Formation Is Not Obvious from LC Traces.

Supplemental Figure 5. Other Asx Residues in the PRH75 Are Susceptible to IsoAsp Formation Due to Heat Treatment.

Supplemental Figure 6. Recombinant PIMT Does Not Influence RNA Duplex Stability or Formation.

Supplemental Figure 7. Presumptive Mutant Seeds of the SALK_060686 Line Do Not Arrest at a Well-Defined Stage of Development.

ACKNOWLEDGMENTS

We thank Lynnette Dirk for PRH75 protein purification for CD and GeneMANIA investigations. David Rodgers and Trevor Creamer kindly provided access to, and instruction in the use of, the Jasco J-810 spectropolarimeter housed in the UK Center for Structural Biology and the COBRE Protein Analytical Core (U.S. Public Health Services Grant P20GM103486). Martin Chow kindly provided instruction on the use of the same instrument and assisted with its setup and data retrieval. All three provided expert advice on the interpretation of CD spectra and thermal denaturation curves. We also thank David Martin, Venkata Krishna Doppalapudi, and Kim R. Schäfermeyer for excellent technical assistance during this project. This research was conducted under the auspices of National Science Foundation Grant 0449649 (A.B.D. and S. G.C.), National Institutes of Health Grant GM58843 (P.A.L.), and National Institutes of Health Grant GM026020 (S.G.C.). Two anonymous reviewers improved the clarity of the article.

AUTHOR CONTRIBUTIONS

N.R.N. and A.A.P. conducted the PRH75 helicase unwinding assays, PRH75 characterization, and rescue by PIMT and helped write the article. B.A. and P.A.L. planned and conducted the LC-MS/MS analysis of PRH75 and helped write the article. J.D.L. and S.G.C. planned and conducted the DEAD-box peptide analyses, constructed figures, and helped write the article. T.C. discovered PRH75 isoAsp susceptibility, made PRH75 constructs for protein expression, and helped write the article. E.J. planned the PRH75 helicase and rescue experiments and helped write the article. S.E.P. and R.D.D. recovered the *prh75* homozygous lines complemented with $35S_{pro}$:*PRH75*, characterized the phenotypes from these and the *prh75* mutant, examined embryo lethality, and helped write the article. A.B.D. conceived the project, designed and conducted the PRH75 rewinding experiments, acquired scanning electron micrographs, conducted the CD analysis, and helped write the article.

Received May 6, 2013; revised June 28, 2013; accepted July 9, 2013; published July 31, 2013.

REFERENCES

Alonso, J.M., et al. (2003). Genome-wide insertional mutagenesis of *Arabidopsis thaliana*. Science **301:** 653–657.

An, Y.Q., and Lin, L. (2011). Transcriptional regulatory programs underlying barley germination and regulatory functions of gibberellin and abscisic acid. BMC Plant Biol. **11:** 105.

Bork, P., and Koonin, E.V. (1993). An expanding family of helicases within the 'DEAD/H' superfamily. Nucleic Acids Res. **21:** 751–752.

Brown, A.M. (2001). A step-by-step guide to non-linear regression analysis of experimental data using a Microsoft Excel spreadsheet. Comput. Methods Programs Biomed. **65:** 191–200.

Chen, J., Edwards, S.A., Grater, F., and Baldauf, C. (2012). On the cis to trans isomerization of prolyl-peptide bonds under tension. J. Phys. Chem. **116:** 9346–9351.

Chen, T., et al. (2010). Substrates of the *Arabidopsis thaliana* protein isoaspartyl methyltransferase 1 identified using phage display and biopanning. J. Biol. Chem. **285:** 37281–37292.

Cloos, P.A., and Christgau, S. (2002). Non-enzymatic covalent modifications of proteins: Mechanisms, physiological consequences and clinical applications. Matrix Biol. **21:** 39–52.

Clough, S.J., and Bent, A.F. (1998). Floral dip: A simplified method for Agrobacterium-mediated transformation of *Arabidopsis thaliana*. Plant J. **16:** 735–743.

Cordin, O., Banroques, J., Tanner, N.K., and Linder, P. (2006). The DEAD-box protein family of RNA helicases. Gene **367:** 17–37.

Desfougères, Y., Jardin, J., Lechevalier, V., Pezennec, S., and Nau, F. (2011). Succinimidyl residue formation in hen egg-white lysozyme favors the formation of intermolecular covalent bonds without affecting its tertiary structure. Biomacromolecules **12:** 156–166.

Fairman-Williams, M.E., Guenther, U.P., and Jankowsky, E. (2010). SF1 and SF2 helicases: Family matters. Curr. Opin. Struct. Biol. **20:** 313–324.

Galat, A. (1993). Peptidylproline cis-trans-isomerases: Immunophilins. Eur. J. Biochem. **216:** 689–707.

He, D., Han, C., Yao, J., Shen, S., and Yang, P. (2011). Constructing the metabolic and regulatory pathways in germinating rice seeds through proteomic approach. Proteomics **11:** 2693–2713.

Jankowsky, E., and Fairman, M.E. (2007). RNA helicases—One fold for many functions. Curr. Opin. Struct. Biol. **17:** 316–324.

Jankowsky, E., and Putnam, A. (2010). Duplex unwinding with DEAD-box proteins. Methods Mol. Biol. **587:** 245–264.

Johnston, A.J., Meier, P., Gheyselinck, J., Wuest, S.E., Federer, M., Schlagenhauf, E., Becker, J.D., and Grossniklaus, U. (2007). Genetic subtraction profiling identifies genes essential for *Arabidopsis* reproduction and reveals interaction between the female gametophyte and the maternal sporophyte. Genome Biol. **8:** R204.

Kelly, S.M., Jess, T.J., and Price, N.C. (2005). How to study proteins by circular dichroism. Biochim. Biophys. Acta **1751:** 119–139.

Kelly, S.M., and Price, N.C. (2000). The use of circular dichroism in the investigation of protein structure and function. Curr. Protein Pept. Sci. **1:** 349–384.

Kern, D., Schutkowski, M., and Drakenberg, T. (1997). Rotational barriers of cis/trans isomerization of proline analogues and their catalysis by cyclophilin. J. Am. Chem. Soc. **119:** 8403–8408.

Kimura, M., and Nambara, E. (2010). Stored and neosynthesized mRNA in *Arabidopsis* seeds: Effects of cycloheximide and controlled deterioration treatment on the resumption of transcription during imbibition. Plant Mol. Biol. **73:** 119–129.

Klassen, T.L., O'Mara, M.L., Redstone, M., Spencer, A.N., and Gallin, W.J. (2008). Non-linear intramolecular interactions and voltage sensitivity of a KV1 family potassium channel from *Polyorchis penicillatus* (Eschscholtz 1829). J. Exp. Biol. **211:** 3442–3453.

Kobayashi, K., Otegui, M.S., Krishnakumar, S., Mindrinos, M., and Zambryski, P. (2007). *INCREASED SIZE EXCLUSION LIMIT2* encodes a putative DEVH box RNA helicase involved in plasmodesmata function during *Arabidopsis* embryogenesis. Plant Cell **19:** 1885–1897.

Koonin, E.V. (1993). A common set of conserved motifs in a vast variety of putative nucleic acid-dependent ATPases including MCM proteins involved in the initiation of eukaryotic DNA replication. Nucleic Acids Res. **21:** 2541–2547.

Kushwaha, R., Lloyd, T.D., Schäfermeyer, K.R., Kumar, S., and Downie, A.B. (2012). Identification of Late Embryogenesis Abundant (LEA) protein putative interactors using phage display. Int. J. Mol. Sci. **13:** 6582–6603.

Kushwaha, R., Payne, C.M., and Downie, A.B. (2013). Uses of phage display in Agriculture: A review of food-related protein-protein interactions discovered by affinity selection over diverse baits. Comp. Math. Meth. Med. **2013:** 12.

Li, S.C., Chung, M.C., and Chen, C.S. (2001). Cloning and characterization of a DEAD box RNA helicase from the viable seedlings of aged mung bean. Plant Mol. Biol. **47:** 761–770.

Lorković, Z.J., Herrmann, R.G., and Oelmüller, R. (1997). PRH75, a new nucleus-localized member of the DEAD-box protein family from higher plants. Mol. Cell. Biol. **17:** 2257–2265.

Lorković, Z.J., Hilscher, J., and Barta, A. (2004). Use of fluorescent protein tags to study nuclear organization of the spliceosomal machinery in transiently transformed living plant cells. Mol. Biol. Cell **15:** 3233–3243.

Lowenson, J.D., and Clarke, S. (1991). Structural elements affecting the recognition of L-isoaspartyl residues by the L-isoaspartyl/D-aspartyl protein methyltransferase. Implications for the repair hypothesis. J. Biol. Chem. **266:** 19396–19406.

Lowry, O.H., Rosebrough, N.J., Farr, A.L., and Randall, R.J. (1951). Protein measurement with the Folin phenol reagent. J. Biol. Chem. **193:** 265–275.

MacLaren, D.C., and Clarke, S. (1995). Expression and purification of a human recombinant methyltransferase that repairs damaged proteins. Protein Expr. Purif. **6:** 99–108.

Meinke, D., Muralla, R., Sweeney, C., and Dickerman, A. (2008). Identifying essential genes in *Arabidopsis thaliana*. Trends Plant Sci. **13:** 483–491.

Meinke, D.W. (1994). Seed development in *Arabidopsis thaliana*. In *Arabidopsis*, E.M. Meyerowitz and C.R. Somerville, eds (Cold Spring Harbor, NY: Cold Spring Harbor Laboratory Press), pp. 253–295.

Mingam, A., Toffano-Nioche, C., Brunaud, V., Boudet, N., Kreis, M., and Lecharny, A. (2004). DEAD-box RNA helicases in *Arabidopsis thaliana*: Establishing a link between quantitative expression, gene structure and evolution of a family of genes. Plant Biotechnol. J. **2:** 401–415.

O'Connor, P.B., Cournoyer, J.J., Pitteri, S.J., Chrisman, P.A., and McLuckey, S.A. (2006). Differentiation of aspartic and isoaspartic acids using electron transfer dissociation. J. Am. Soc. Mass Spectrom. **17:** 15–19.

Ogé, L., Bourdais, G., Bove, J., Collet, B., Godin, B., Granier, F., Boutin, J.P., Job, D., Jullien, M., and Grappin, P. (2008). Protein repair L-isoaspartyl methyltransferase 1 is involved in both seed longevity and germination vigor in *Arabidopsis*. Plant Cell **20:** 3022–3037.

Pagnussat, G.C., Yu, H.J., Ngo, Q.A., Rajani, S., Mayalagu, S., Johnson, C.S., Capron, A., Xie, L.F., Ye, D., and Sundaresan, V. (2005). Genetic and molecular identification of genes required for female gametophyte development and function in *Arabidopsis*. Development **132:** 603–614.

Pyle, A.M. (2008). Translocation and unwinding mechanisms of RNA and DNA helicases. Annu. Rev. Biophys. **37:** 317–336.

Rajjou, L., Duval, M., Gallardo, K., Catusse, J., Bally, J., Job, C., and Job, D. (2012). Seed germination and vigor. Annu. Rev. Plant Biol. **63:** 507–533.

Rajjou, L., Gallardo, K., Debeaujon, I., Vandekerckhove, J., Job, C., and Job, D. (2004). The effect of alpha-amanitin on the *Arabidopsis* seed proteome highlights the distinct roles of stored and neosynthesized mRNAs during germination. Plant Physiol. **134:** 1598–1613.

Rajjou, L., Lovigny, Y., Groot, S.P., Belghazi, M., Job, C., and Job, D. (2008). Proteome-wide characterization of seed aging in *Arabidopsis*: A comparison between artificial and natural aging protocols. Plant Physiol. **148:** 620–641.

Razick, S., Magklaras, G., and Donaldson, I.M. (2008). iRefIndex: A consolidated protein interaction database with provenance. BMC Bioinformatics **9:** 405.

Roberts, E.H. (1973). Predicting the storage life of seeds. Seed Science and Technology **1:** 499–514.

Rocak, S., and Linder, P. (2004). DEAD-box proteins: The driving forces behind RNA metabolism. Nat. Rev. Mol. Cell Biol. **5:** 232–241.

Rogers, G.W., Jr., Richter, N.J., and Merrick, W.C. (1999). Biochemical and kinetic characterization of the RNA helicase activity of eukaryotic initiation factor 4A. J. Biol. Chem. **274:** 12236–12244.

Sallon, S., Solowey, E., Cohen, Y., Korchinsky, R., Egli, M., Woodhatch, I., Simchoni, O., and Kislev, M. (2008). Germination, genetics, and growth of an ancient date seed. Science **320:** 1464.

Schwartz, B.W., Yeung, E.C., and Meinke, D.W. (1994). Disruption of morphogenesis and transformation of the suspensor in abnormal suspensor mutants of *Arabidopsis*. Development **120:** 3235–3245.

Shen-Miller, J., Mudgett, M.B., Schopf, J.W., Clarke, S., and Berger, R. (1995). Exceptional seed longevity and robust growth: Ancient sacred lotus from China. Am. J. Bot. **82:** 1367–1380.

Tzafrir, I., Pena-Muralla, R., Dickerman, A., Berg, M., Rogers, R., Hutchens, S., Sweeney, T.C., McElver, J., Aux, G., Patton, D., and Meinke, D. (2004). Identification of genes required for embryo development in *Arabidopsis*. Plant Physiol. **135:** 1206–1220.

Verma, P., Kaur, H., Petla, B.P., Rao, V., Saxena, S.C., and Majee, M. (2013). PROTEIN L-ISOASPARTYL METHYLTRANSFERASE2 is differentially expressed in chickpea and enhances seed vigor and longevity by reducing abnormal isoaspartyl accumulation predominantly in seed nuclear proteins. Plant Physiol. **161:** 1141–1157.

Wang, H., Hill, K., and Perry, S.E. (2004). An *Arabidopsis* RNA lariat debranching enzyme is essential for embryogenesis. J. Biol. Chem. **279:** 1468–1473.

Warde-Farley, D., et al. (2010). The GeneMANIA prediction server: Biological network integration for gene prioritization and predicting gene function. Nucleic Acids Res. **38** (Web Server issue)**:** W214–W220.

Wedemeyer, W.J., Welker, E., and Scheraga, H.A. (2002). Proline cis-trans isomerization and protein folding. Biochemistry **41:** 14637–14644.

Yang, H., and Zubarev, R.A. (2010). Mass spectrometric analysis of asparagine deamidation and aspartate isomerization in polypeptides. Electrophoresis **31:** 1764–1772.

Yang, Q., Fairman, M.E., and Jankowsky, E. (2007). DEAD-box-protein-assisted RNA structure conversion towards and against thermodynamic equilibrium values. J. Mol. Biol. **368:** 1087–1100.

Yang, Q., and Jankowsky, E. (2005). ATP- and ADP-dependent modulation of RNA unwinding and strand annealing activities by the DEAD-box protein DED1. Biochemistry **44:** 13591–13601.

A

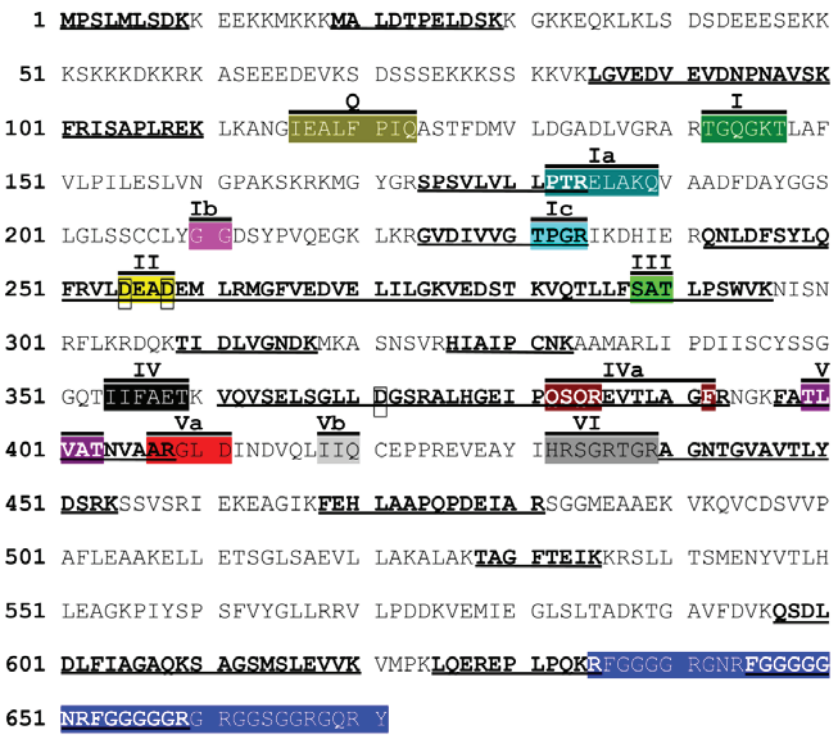

B

Start - End	Observed	Mr(expt)	Mr(calc)	Delta	Sequence
1 - 13	468.8413	1403.5020	1403.7330	-0.2309	MPSLMLSDKKEEK.K
19 - 29	610.1743	1218.3341	1218.5802	-0.2461	K.MALDTPELDSK.K
85 - 102	663.3343	1986.9810	1987.0011	-0.0200	K.LGVEDVEVDNPNAVSKFR.I
103 - 110	457.1619	912.3093	912.5392	-0.2299	R.ISAPLREK.L
174 - 184	591.4117	1180.8088	1180.7180	0.0908	R.SPSVLVLLPTR.E
224 - 234	535.2455	1068.4765	1068.5928	-0.1163	R.GVDIVVGTPGR.I
242 - 252	715.8467	1429.6789	1429.6990	-0.0201	R.QNLDFSYLQFR.V
253 - 262	595.7356	1189.4566	1189.5649	-0.1083	R.VLDEADEMLR.M
263 - 275	725.4123	1448.8246	1448.7585	0.0661	R.MGFVEDVEILGK.V
276 - 281	339.6454	677.3379	677.3231	0.0148	K.VEDSTK.V
282 - 296	845.5036	1688.9927	1688.9501	0.0426	K.VQTLLFSATLPSWVK.N
309 - 316	487.7876	973.5427	973.5080	0.0146	K.TIDLVGNDK.M
326 - 333	476.7348	951.4551	951.4960	-0.0409	R.HIAIPCNK.A carbamidomethyl(C)
361 - 374	730.3475	1458.6804	1458.7678	-0.0874	K.VQVSELSGLLDGSR.A
375 - 385	618.3580	1234.7015	1234.6418	0.0597	R.ALHGEIPQSQR.E
386 - 393	446.6490	891.2834	891.4814	-0.1980	R.EVTLAGFR.N
397 - 408	617.2817	1232.5488	1232.6877	-0.1389	K.FATLVATNVAAR.G
440 - 453	712.3199	1422.6253	1422.7103	-0.0850	R.AGNTGVAVTLYDSR.K
440 - 454	517.9215	1550.7427	1550.8053	-0.0626	R.AGNTGVAVTLYDSRK.S
468 - 481	532.0350	1593.0833	1592.7947	0.2886	K.FEHLAAPQPDEIAR.S
528 - 535	433.6728	865.3310	865.4545	-0.1235	K.TAGFTEIK.K
597 - 609	703.2796	1404.5447	1404.7249	-0.1802	K.QSDLDLFIAGAQK.S
610 - 620	554.2520	1106.4895	1106.5641	-0.0746	K.SAGSMSLEVVK.V
625 - 635	465.3610	1393.0611	1392.7837	0.2773	K.LQEREPLPQKR.F
645 - 659	437.2406	1308.6999	1308.6072	0.0927	R.FGGGGGNRFGGGGGR.G

Supplemental Figure 1. Typical LC-ETD-MS/MS analysis of tryptic peptides of PRH75.

A) Amino acid sequence of PRH75 and representation of sequence coverage by MS/MS analysis as shown in underlined, bold type. The 13 motifs characteristic of DEAD-box helicases are designated by the motif acronym, different color highlight, and a solid black line above the amino acids comprising the motif. The variable, glycine/arginine-rich, carboxy-terminal extension involved in duplex rewinding is highlighted in royal blue. The three aspartates identified as converting to isoAsp in LC-MS/MS analysis are boxed. B) Observed tryptic peptides in a typical analysis arranged from N- to C-terminus. The observed tryptic peptides are shown by their position, experimentally observed *m/z* values, monoisotopic mass (Mr expt), theoretically calculated (Mr calculated) values along with the observed difference (delta) and sequence.

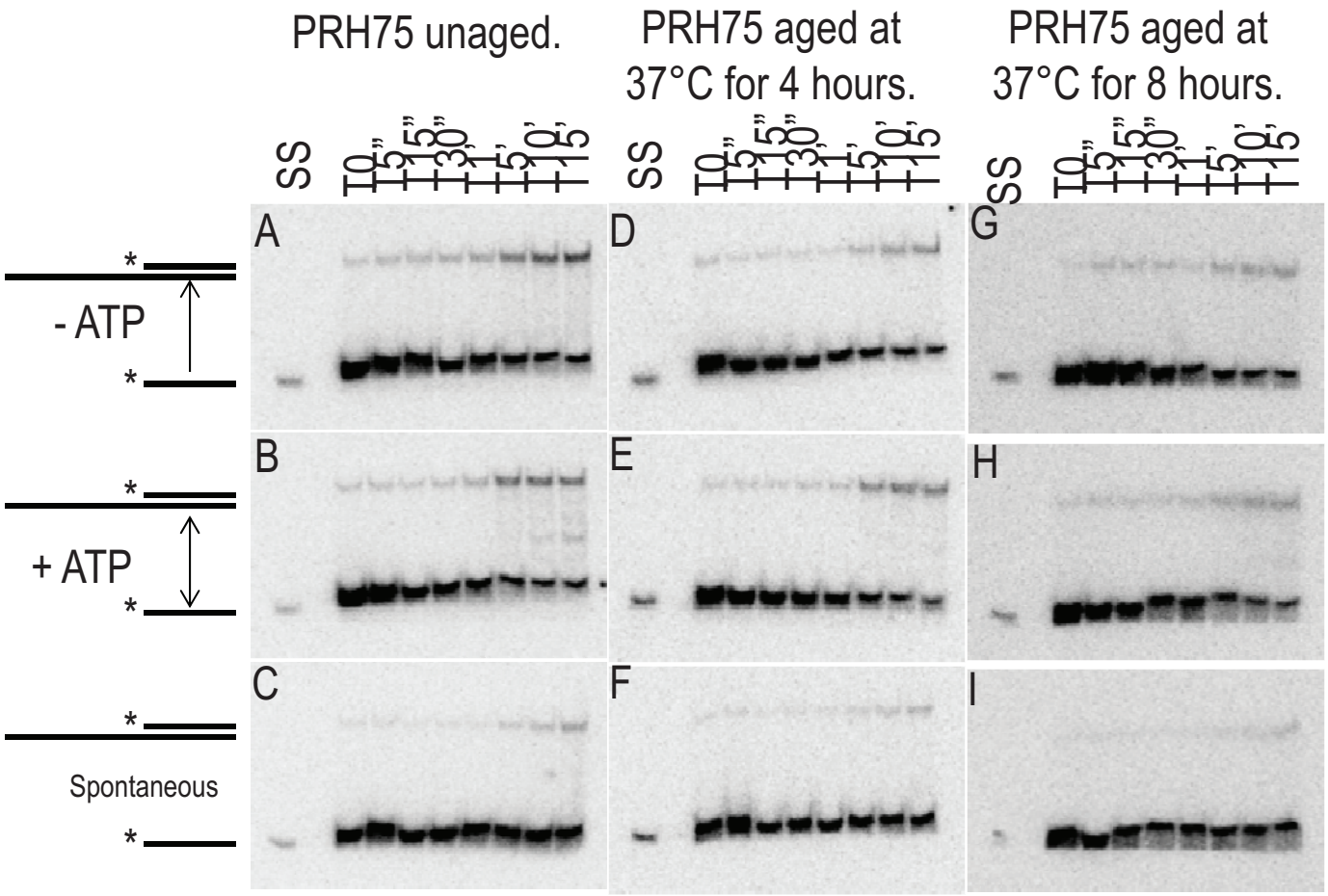

Supplemental Figure 2. Recombinant PRH75 possesses a robust RNA rewinding capacity.
Recombinant PRH75 subjected to 37 °C thermal insult for A-C) 0-, D-F) 4-, or G-I) 8-hours was capable of rewinding a portion of heat-separated RNA strands into a duplex. This rewinding capacity was faster and greater than spontaneous duplex reformation (compare upper two panels for each treatment with the lower one), was present even in 8h thermally insulted enzyme (see G-I), and was evident in unaged samples in the presence of 2 mM ATP where the unwinding reaction was also feasible. Gels were run with an aliquot of the small, single stranded, labeled RNA in the first lane (SS) as a size marker. Rewinding and unwinding reactions were over the time points depicted. Without ATP only the rewinding reaction is anticipated. Spontaneous refers to the self-annealing of the denatured RNA strands without enzyme.

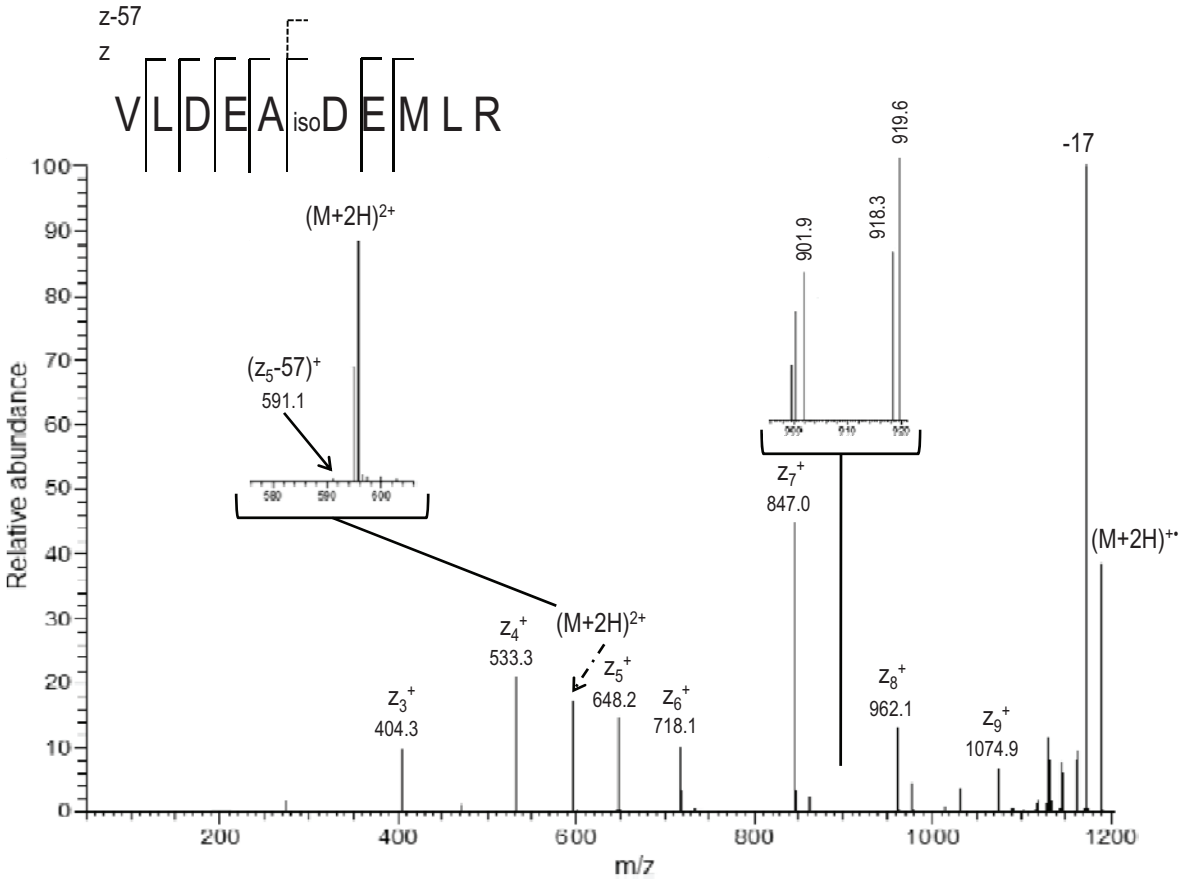

Supplemental Figure 3. The aspartates of the DEAD-box are differentially susceptible to isoAsp formation.

MS/MS spectrum of tryptic peptide VLDEADEMLR from PRH75 exposed to 37 °C for 4 h. Sequence specific fragmentation of the peptide with the z-type product ions were shown in the spectrum. Iso-D diagnostic product ion was observed for aspartate at position 258 (z5-57 at 591.1) but not for position 255 (no z8-57 ion at 905.1) as shown in the expanded regions above the MS/MS spectrum.

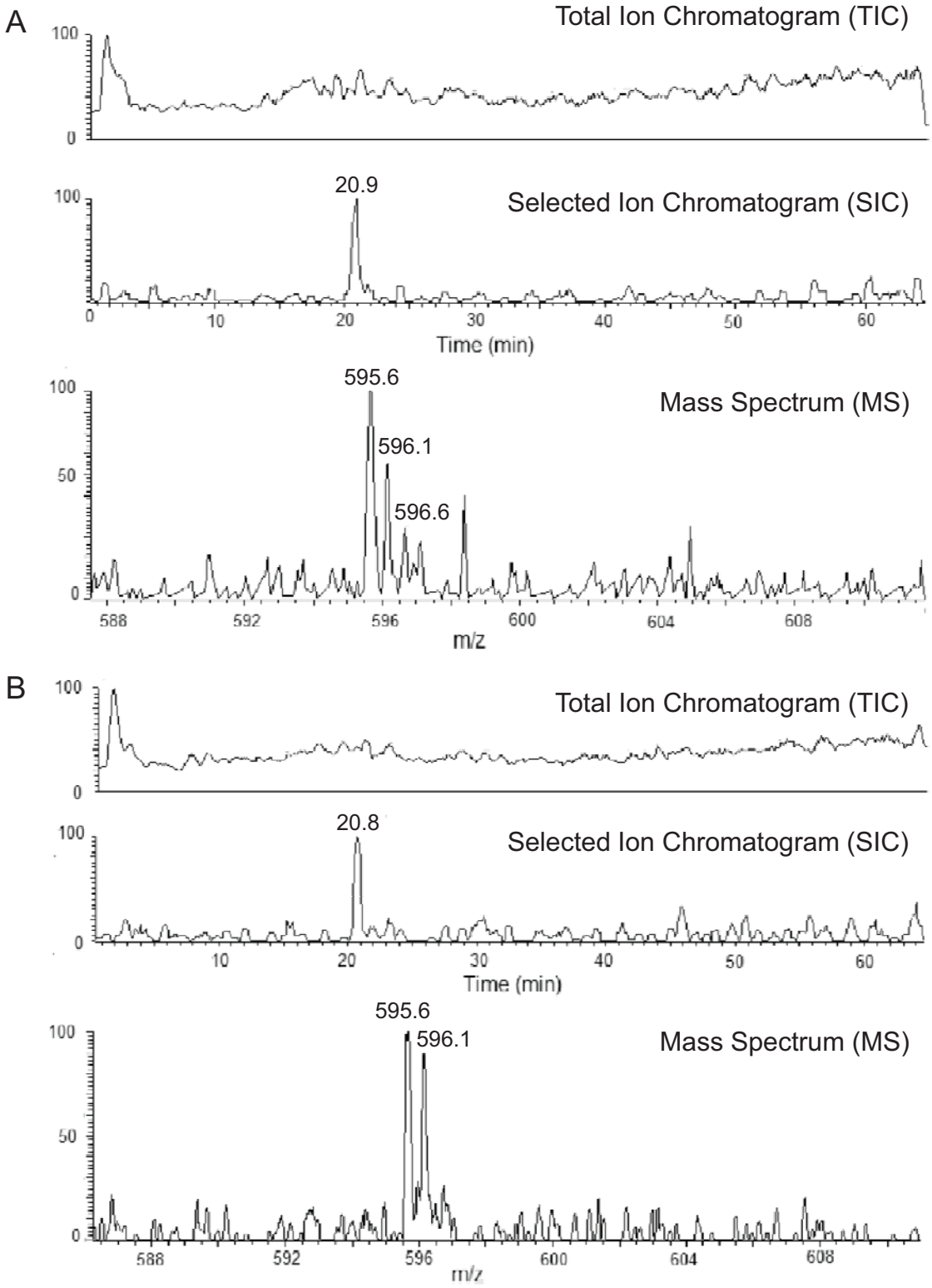

Supplemental Figure 4. IsoAsp formation is not obvious from LC traces.

LC-MS analysis of tryptic peptide VLDEADEMLR (amino acid positions 253-262 of rPRH75) eluting at around 20.7 min from a C18 Xbridge column. Representation of the peptide from A) PRH75 treated at 25°C for 36 h, and B) PRH75 exposed to 37°C for 12 h prior to trypsin treatment at 25°C. The total ion current (TIC), selected ion current (SIC) for *m/z* 595.66, and the mass spectrum (MS) highlighting the doubly charged peptide *m/z* 595.64/595.68 is shown.

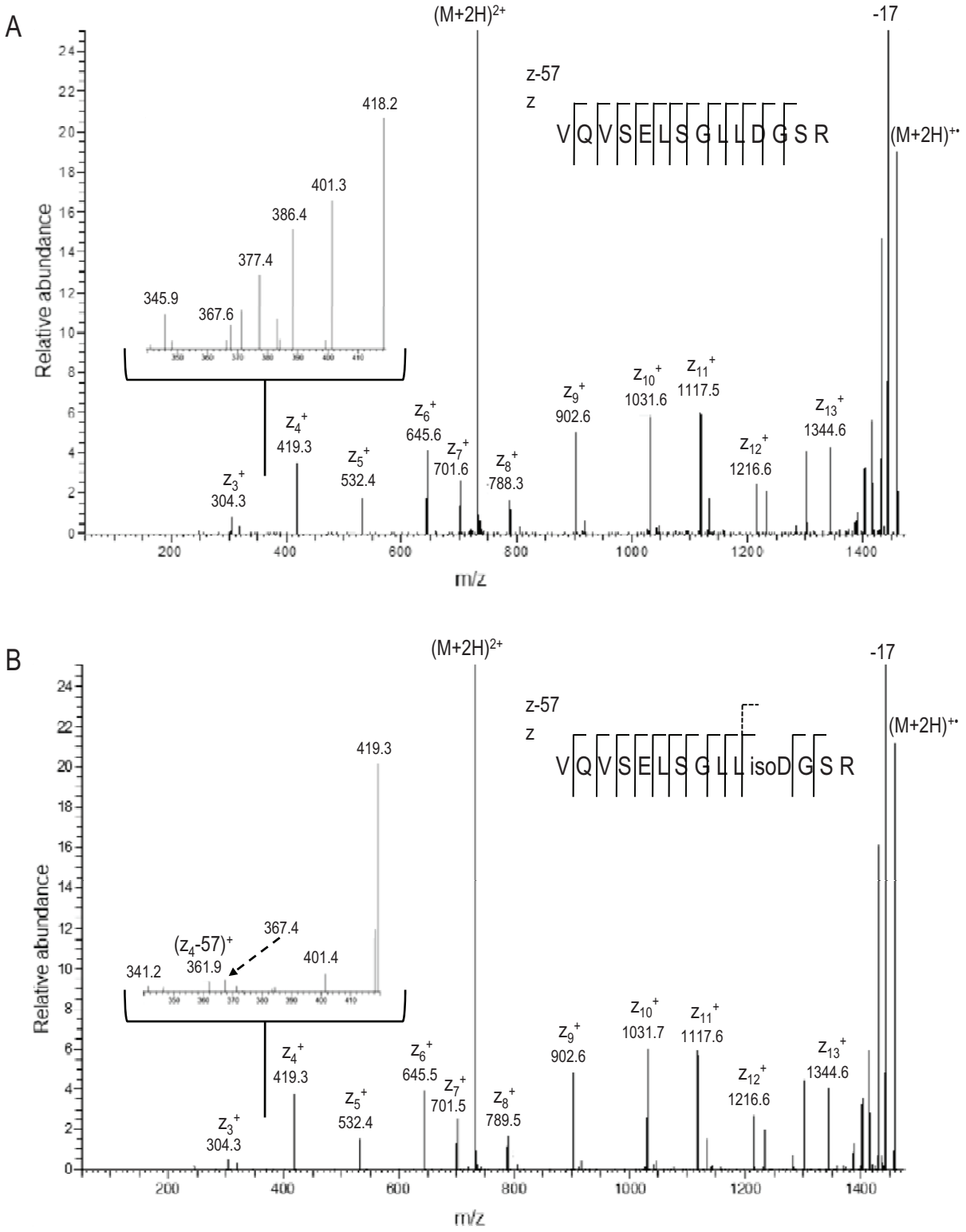

Supplemental Figure 5. Other Asx residues in the PRH75 are susceptible to isoAsp formation due to heat treatment.

MS/MS spectra of tryptic peptide VQVSELSGLLDGSR (amino acid positions 361-374) eluting at 28.4 minutes from C18 column. Peptide resulting from exposure of rPRH75 at 25 °C for A) 36 h is compared against the sample exposed at 37°C for B) 12 h. Sequence specific fragmentation of the peptide with the z-type product ions are shown in the spectrum. Absence or presence of iso-D diagnostic product ion for aspartate at position 371 (z4-57 at 362.3) is shown in expanded region above the MS/MS spectrum.

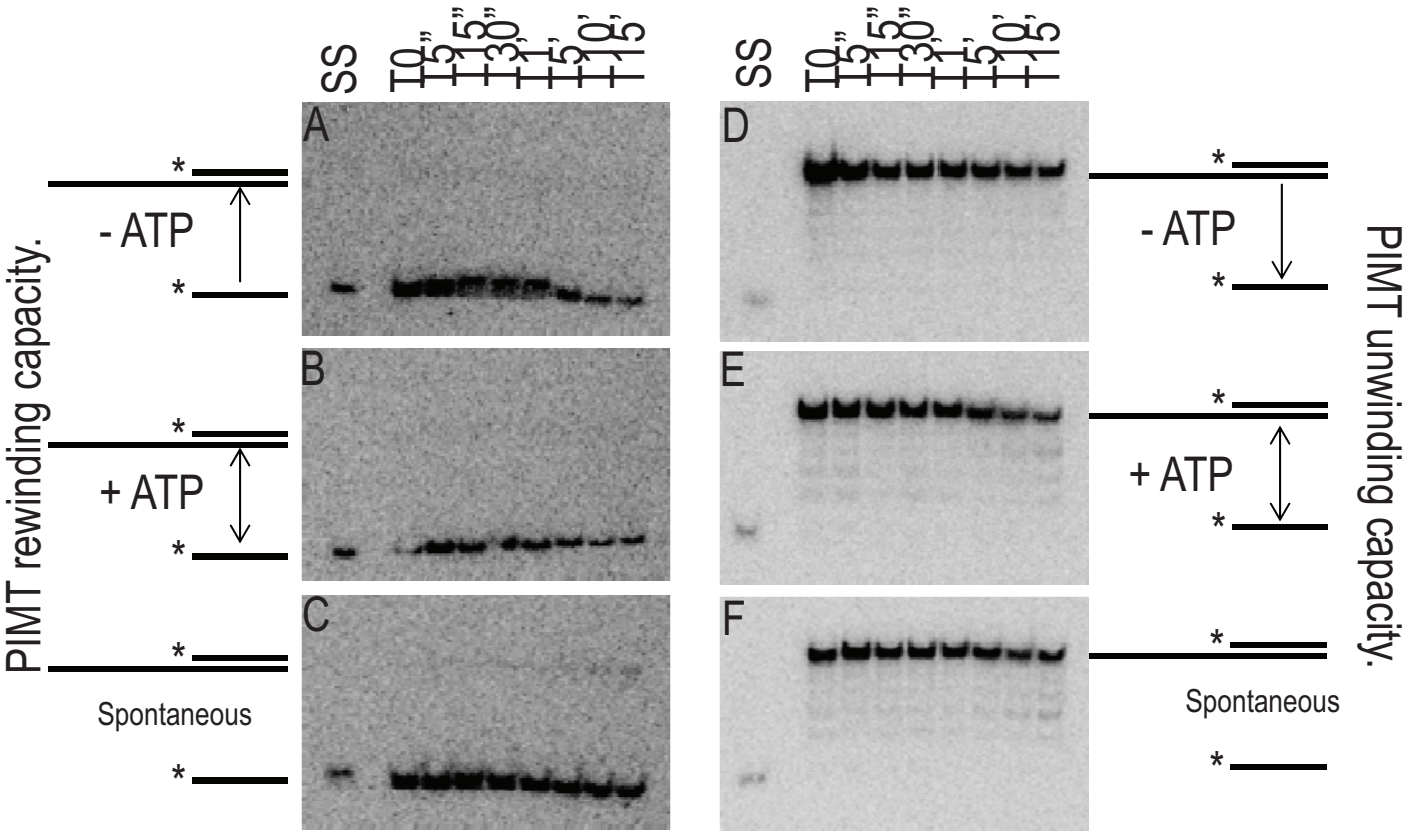

Supplemental Figure 6. Recombinant PIMT does not influence RNA duplex stability or formation. PIMT alone (without PRH75) exhibited neither a rewinding nor an unwinding capacity at the same protein concentration as PRH75. Gels were run with an aliquot of the small, single stranded, labeled RNA in the first lane (SS) as a size marker. Rewinding and unwinding reactions were over the time points depicted. Regardless of ATP presence, no unwinding reaction is anticipated. Spontaneous refers to the self-annealing/unwinding of the RNA strands without enzyme.

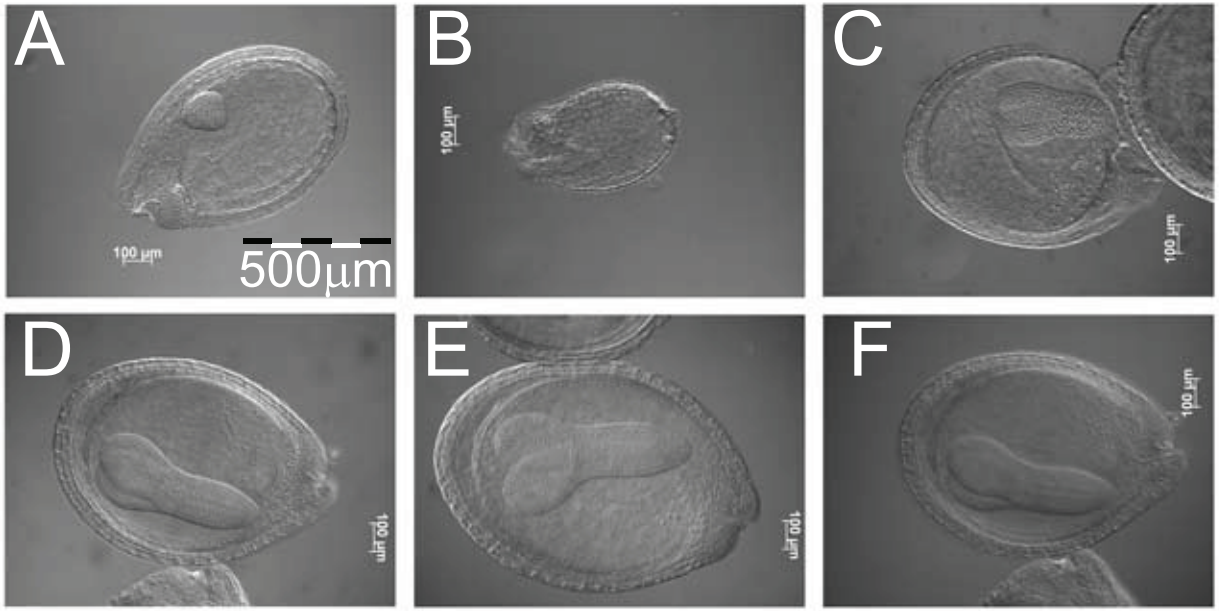

Supplemental Figure 7. Presumptive mutant seeds of the SALK_060686 line do not arrest at a well defined stage of development.

Seeds from a single, green silique from a heterozygous SALK_060686 plant were collected and cleared with Hoyer's solution before being photographed under a microscope. The embryo in seeds of small size and/or of an odd shape and/or color were compared with the embryo in apparently normal looking seeds to determine if there was a specific stage at which SALK_060686 prh75 mutant embryos were arresting. Three presumptive mutant seeds A-C) are depicted as are D-F) three presumably normal seeds. The size of the black and white bar in panel A is 0.5 mm. The scale is the same for all micrographs.